Coordination Chemistry Reviews 252 (2008) 2596–2611

Contents lists available at ScienceDirect

Coordination Chemistry Reviews

journal homepage: www.elsevier.com/locate/ccr

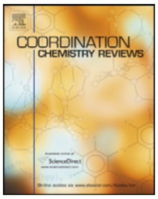

Review

Optimising the luminescence of platinum(II) complexes and their application in organic light emitting devices (OLEDs)☆

J.A. Gareth Williams*, Stéphanie Develay, David L. Rochester, Lisa Murphy

Department of Chemistry, University of Durham, Durham DH1 3LE, UK

Contents

ARTICLE INFO

Article history:
Received 2 January 2008
Accepted 16 March 2008
Available online 7 April 2008

Keywords:
Platinum
Photochemistry
Luminescence
Electroluminescence
OLEDs

ABSTRACT

In this contribution, we provide an overview of some of the strategies for maximising the luminescence efficiencies of simple square-planar platinum(II) complexes in solution, including the introduction of strong-field co-ligands into di- and tri-imine complexes, involvement of intraligand charge-transfer excited states, and cyclometallation. We then explore in more detail several classes of platinum(II) complexes containing cyclometallating bidentate and terdentate ligands, many of which are significantly luminescent in solution at room temperature. The background to the use of brightly emissive platinum(II) complexes as phosphors in organic light emitting devices (OLEDs) is discussed. Key recent studies on the use of Pt(II) complexes in OLEDs are reviewed.

☆ ISPPCC-17 contribution.

* Corresponding author. Tel.: +44 191 334 2124; fax: +44 191 384 4737.
E-mail address: j.a.g.williams@durham.ac.uk (J.A. Gareth Williams).

0010-8545/$ – see front matter © 2008 Elsevier B.V. All rights reserved.
doi:10.1016/j.ccr.2008.03.014

1. Introduction and scope

In the 1970s and 1980s, the development of new platinum(II) complexes was driven primarily by two distinct themes, namely the emerging unprecedented success of *cis*-$Pt(NH_3)_2Cl_2$ (cisplatin) as an anticancer agent, and research into one-dimensional, electrically conducting molecular materials exploiting the stacking interactions between square-planar complexes [1,2]. The past decade has seen attention turn increasingly to the excited state properties of platinum(II) complexes, amongst which luminescence occupies a central position. Twenty years ago, a number of simple platinum(II) complexes were known that emit in the solid state or at low temperature, but almost none that were significantly luminescent in solution under ambient conditions [3]. A number of investigations since that time have helped to provide an understanding of the factors that govern the luminescence efficiencies of platinum(II) complexes [4]. A key contemporary driving force for research in this area is the application of luminescent transition metal complexes as phosphors in organic light emitting devices (OLEDs) [5]. In this review, we first present an overview of the factors that need to be taken into account in the rational design of highly emissive platinum(II) complexes, and then consider in more detail the properties of several classes of cyclometallated compounds that are luminescent in solution, including some key highlights on the application of such compounds to OLED technology from the past 5 years.

2. Optimising the luminescence of platinum(II) complexes

2.1. Factors determining the luminescence quantum yield of platinum(II) complexes

As for any other fluorescent molecule, optimising the luminescence efficiency of platinum(II) complexes requires that the radiative rate constant k_r of the emissive state be promoted while the rates of non-radiative decay pathways, $\sum k_{nr}$, are minimised. Assuming that the emissive state is formed with unitary efficiency, then the quantum yield Φ_{lum} is determined by these parameters through Eq. (1):

$$\Phi_{lum} = \frac{k_r}{k_r + \sum k_{nr}} \tag{1}$$

In the case of simple platinum(II) complexes with relatively small ligands, where the metal orbitals make a significant contribution to the excited states, the high spin–orbit coupling constant of Pt ($\chi = 4481\ cm^{-1}$ [6]) promotes rapid intersystem crossing from singlet to triplet states, at a rate probably of the order of $10^{12}\ s^{-1}$ [7]. Since this greatly exceeds typical radiative rate constants of singlet excited states, emission normally emanates from states of triplet character (unless the excited state is localised on a remote part of the ligand well removed from the metal centre [8]), and the assumption that the emissive state is formed with approximately unitary efficiency is essentially valid.

2.1.1. Radiative decay

The subsequent radiative decay of the triplet state, which is formally forbidden in purely organic systems (k_r typically in the range 10^{-1} to $10^2\ s^{-1}$), should be promoted by the high spin–orbit coupling constant of Pt(II). The extent to which this occurs – one of the two key factors that determines the overall quantum yields of emission – depends on the contribution of metal orbitals to the lowest-energy triplet excited state: k_r values are expected to be highest for those states comprising significant metal character.

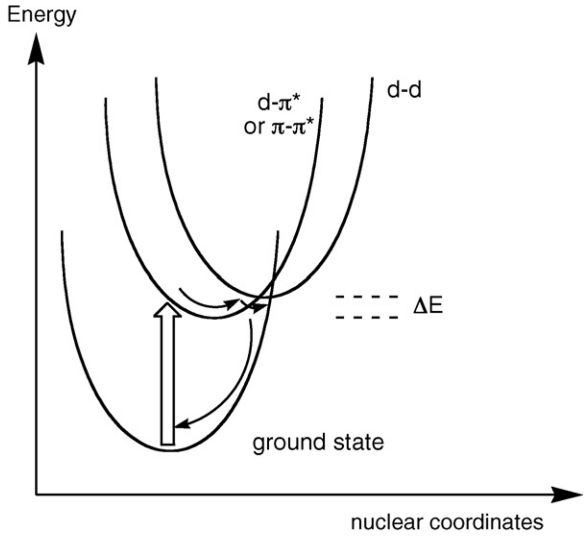

Fig. 1. The potential energy surface of the d–d excited state in Pt(II) complexes is displaced relative to the ground state, owing to the strongly antibonding character of the d_{x2-y2} orbital that is populated. Although other states (e.g. d–π* or π–π*) may lie at lower energies, the d–d state can provide a thermally activated pathway of non-radiative decay. Thick arrow represents absorption of light; thin ones indicate vibrational relaxation and non-radiative decay.

2.1.2. Non-radiative decay

The strong preference of Pt(II) complexes to be square planar, owing to ligand field stabilisation, results in the unoccupied d_{x2-y2} orbital being strongly antibonding. Population of this orbital will be accompanied by elongation of Pt–L bonds and severe distortion, promoting non-radiative decay of metal-centred (d–d) excited states to the ground state at the isoenergetic crossing point of the potential energy surfaces. Even if excited states of different character, such as MLCT (d–π*) or LC (π–π*) states, lie at lower energies than the d–d states, the latter can still exert a deleterious influence if they are thermally accessible, i.e. if ΔE is comparable to kT (Fig. 1). For example, in contrast to the archetypal luminescent complex $[Ru(bpy)_3]Cl_2$ that emits from a ^{3}MLCT state, the corresponding excited state of the related platinum complex $[Pt(bpy)Cl_2]$ is non-emissive in solution at room temperature, owing to thermally activated non-radiative decay via the d–d state [9]. A similar process probably accounts for the lack of room temperature emission from the *bis*-bipyridyl ruthenium(II) complex $Ru(bpy)_2Cl_2$.

2.2. Strategies for promoting luminescence in platinum(II) complexes

It is clear from the above discussion that, in order to promote emission in solution at ambient temperature, it is necessary to ensure that (i) the lowest-lying excited state is *not* a metal-centred d–d state but rather a ligand-centred or charge-transfer state; and (ii) there is a large energy gap, ΔE, between the lowest-lying excited state and higher-lying d–d state, such that thermally activated depopulation via the latter is inhibited. There are two ways to increase ΔE, namely to lower the energy of the emitting state or to raise that of the d–d state.

2.2.1. Low energy emitting states

A classic example is the platinum porphyrins. For example, platinum octaethylporphyrin (PtOEP) **1** emits deep into the red region with high quantum yield, $\lambda_{max} = 641$ nm, $\tau = 65\ \mu s$, $\Phi_{lum} = 0.6$ [10]; the rigidity of porphyrinic complexation also helps here, of course. In the case of polypyridyl ligands, on the other hand, pendent aryl substituents can induce beneficial effects [11]. A striking recent example is provided by McMillin and co-workers [12]. They have found that, whilst $[Pt(tpy)Cl]^+$ is non-emissive in solution at RT, electron-rich pendants on the terpyridine introduce low-energy ^{1,3}ILCT states that can be significantly emissive at room temperature; for $[Pt\{4'\text{-(pyren-1-yl)-tpy}\}Cl]^+$, λ_{max} = 685 nm, τ = 6.4 μs, Φ_{lum} = 0.034 in CH_2Cl_2 at RT [8,13].

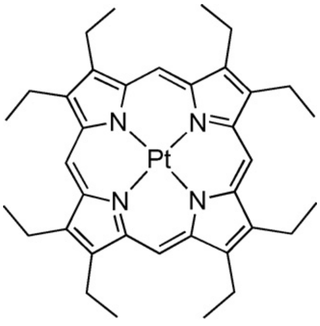

PtOEP

1

2.2.2. *Raising the energy of d–d states*

In order to push up d–d states to high energies to try to make them thermally inaccessible, strong-field ligands or co-ligands can be introduced. The substitution of weak-field halide ligands by strong-field cyanides provides an example of how an increase in the ligand field strength of the ancillary ligand promotes luminescence: several $[Pt(N\hat{}N)(CN)_2]$ complexes emit in solution at room temperature, whereas the corresponding chloro complexes normally do not; e.g. for $Pt(5,5'\text{-}Me_2\text{-bpy})(CN)_2$, $\Phi \sim 10^{-3}$ [14], and for $[Pt(tpy)CN]^+$, $\Phi_{lum} = 4 \times 10^{-4}$ [15]. The downside of the cyanide ligand, however, is that it may lead to a switch in the nature of the emissive state from MLCT to LC, by lowering the energy of the highest filled metal-centred orbital. The lower contribution of metal character to the emissive state compromises k_r, leading to the disappointingly low quantum yields observed.

Acetylide co-ligands, R–C≡C–, prove more successful, and a large number of platinum(II) di- and tri-imine complexes containing two or one acetylides, respectively, have been discovered over the past decade that are luminescent at RT. As for X = –C≡N, the strong-field acetylide ligand raises the energy of the d–d states, diminishing $\sum k_{nr}$. However, the R–C≡C– ligand is more strongly donating than CN^-, which helps to ensure significant metal character in the HOMO, and hence larger radiative rate constants k_r. Overall, therefore, such complexes are often quite strongly emissive in fluid solution at room temperature [16–23]. The subject has been reviewed by Castellano et al. in the preceding ISPPCC edition of this journal [24].

A further strategy is to make use of cyclometallating ligands that are closely related to bipyridine and terpyridine, but which serve to augment the ligand-field strength without the need for specific co-ligands. It is on such systems – and their applications in OLEDs – that subsequent sections of this review will focus.

3. Introduction to cyclometallated complexes

Cyclometallation refers to the binding of a polydentate ligand to a metal via a covalent metal–carbon bond, the remaining bonds normally being coordinate bonds from heteroatoms such as nitrogen in the ligand. Cyclometallated complexes are thus strictly organometallic compounds. For example, 2-phenylpyridine (ppy) can bind to a variety of 2nd and 3rd row transition metal ions as an N^C ligand, forming a 5-membered chelate through the carbon atom of the phenyl ring which is *ortho* to the link to the pyridine nitrogen (e.g. as in structure **2**). Since the process involves a net deprotonation of the aromatic C–H, cyclometallating ligands like ppy are anionic, rather than neutral like bpy. The C^- ligating atom

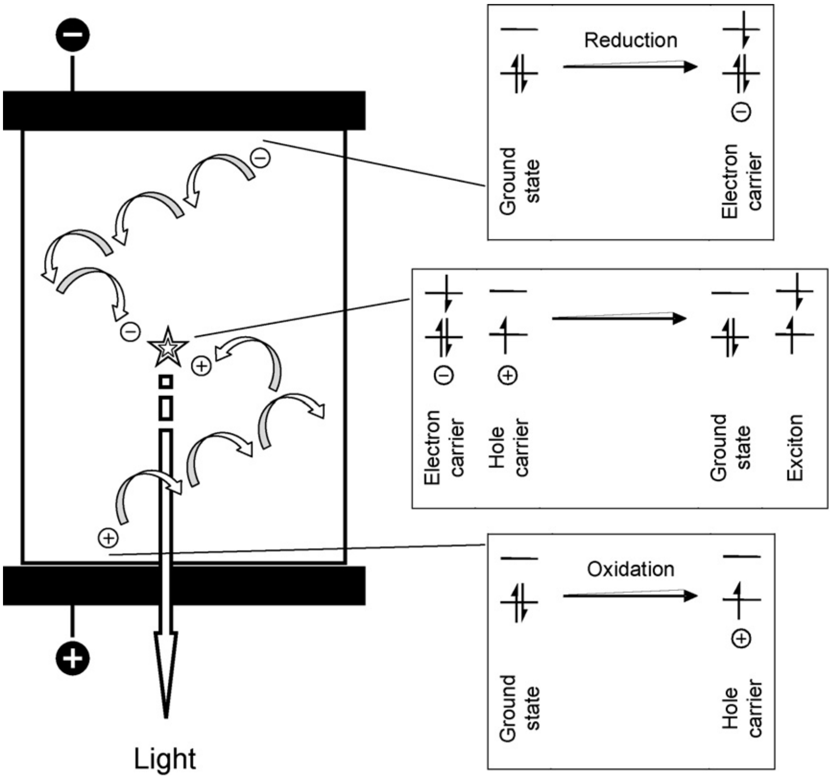

Fig. 2. Schematic representation of electroluminescence in organic materials.

is a very strong σ donor, whilst the pyridyl group remains a good π-acceptor, so that these ligands offer the metal ion a very strong ligand-field. The important consequence for the photophysics and excited state properties is that the energy of deactivating d–d states is raised compared to analogous NˆN complexes, much like the effect of acetylide ligands discussed earlier. Thus, many cyclometallated platinum complexes prove to be luminescent in solution under ambient conditions, some of them intensely so. It is this feature that has led to the recent interest in such compounds as triplet emitters in OLEDs [5].

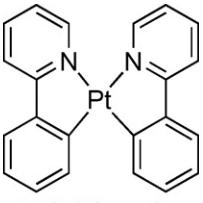
Pt(*N*^*C*-ppy)$_2$

2

4. Organic light emitting devices

In a simple electroluminescent device, an organic emissive layer is sandwiched between two electrodes [25]. Upon application of an electric potential, the organic layer at the cathode is reduced and at the anode oxidised to give electron and hole carriers, respectively (Fig. 2). These migrate under the applied field *via* a hopping mechanism until they either reach the opposite electrode, or meet a charge carrier of the opposite sign. When the latter occurs, the two carriers combine to produce one ground state molecule and an exciton. The nature of this exciton is comparable to the excited state produced by transfer of an electron from the HOMO to LUMO (i.e. the excited S_1 and T_1 states familiar to photoluminescence). Emission of a photon of light from this level then occurs as for photoluminescence.

The combination of charge carriers in an electroluminescent device results in the formation of both singlet and triplet excitons. This contrasts with photoluminescence where, in the absence of significant intersystem crossing, only the excited singlet (S_1) state is populated. Being formally spin-forbidden, phosphorescence from triplet states is rarely observed in organic molecules at RT, and relaxation through non-radiative processes dominates. In an electroluminescent device this results in the generation of unwanted heat. Though often assumed that the formation of excitons is purely statistical with a 25% fraction of singlet excitons due to the 1:3 degeneracies of the singlet and triplet states, this is not necessarily the case, especially as the Pauli exclusion principle reduces electron–electron correlation, resulting in the triplet state being lowered in energy with respect to the singlet state by ∼0.7 eV in both polymeric and small molecular weight materials [26]. However, the unequivocal surplus of triplet states necessarily limits the efficiency of purely organic devices.

4.1. Quantifying the efficiency of OLEDs

A number of parameters are used in reporting the efficiencies of OLEDs, and it is helpful to summarise them briefly here. The fundamental quantity is the internal electroluminescence quantum efficiency, η_{int}, which is defined as the ratio of the number of photons emitted to the number of electrons injected. This is the value most comparable to the PL quantum yield, Φ_{PL}, being the ratio of the number of photons emitted to the number of photons absorbed.

Due to refraction, not all photons produced can escape the bounds of the device. A second quantity, the external EL quantum efficiency η_{ext}, relates the number of photons observed externally to the device to the number of electrons injected. This is related to η_{int} by Eq. (2) where *n* is the refractive index of the organic material.

$$\eta_{\text{int}} = 2n^2\eta_{\text{ext}} \tag{2}$$

Power efficiencies η_{pow} (W W^{-1}) are defined as the ratio of output light power to input electric power. This may be determined from the external EL quantum efficiency by Eq. (3), where E_{p} is the average energy of the emitted photons and *V* is the applied voltage across the device.

$$\eta_{\text{pow}} = \frac{\eta_{\text{ext}}E_{\text{p}}}{V} \tag{3}$$

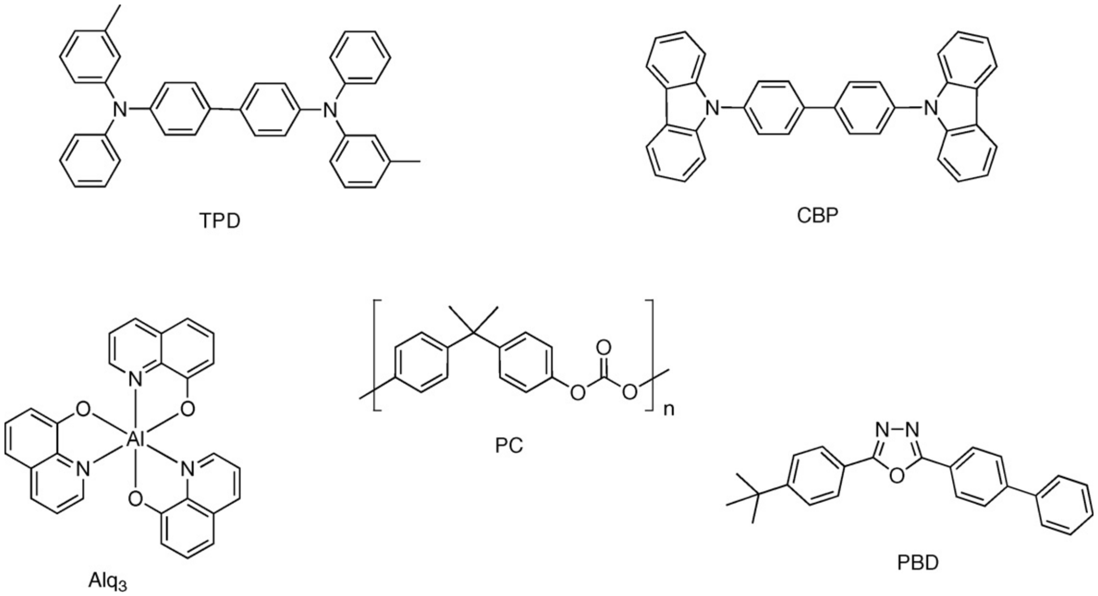

Fig. 3. Structures of some of the materials commonly used as hosts or charge-transporting materials in OLEDs, and referred to in later sections. TPD = *N*,*N*′-bis(3-tolyl)-1,1′-biphenyl-4,4′-diamine; CBP = 4,4′-*N*,*N*′-dicarbazole-biphenyl; Alq$_3$ = tris(8-quinolinolato)aluminum; PC = biphenol-A-polycarbonate; PBD = 2-(4-biphenylyl-5-(4-tertbutylphenyl)-1,2,3-oxadiazole.

While this quantity indicates the power of emitted light, the human eye's sensitivity varies as a function of wavelength, being more sensitive to green light than either red or blue. Another term, the luminous efficiency η_{lum} ($\mathrm{lm\,W^{-1}}$), is determined by applying the eye sensitivity curve S as defined by the Commission Internationale de L'Eclairage (CIE) (Eq. (4)).

$$\eta_{\mathrm{lum}} = \eta_{\mathrm{pow}} S(\lambda) \quad (4)$$

Finally, the brightness of an OLED is often quoted, and specifies the amount of light emitted by a device per unit area ($\mathrm{cd\,m^{-2}}$). A typical laptop display reaches a brightness of about 100 $\mathrm{cd\,m^{-2}}$.

4.2. The role of metal complexes in OLEDs—and the first such devices with platinum porphyrins

By incorporating *phosphorescent* compounds into the emissive layer, emission can occur from both singlet and triplet excitons, and 100% internal EL quantum efficiency can potentially be achieved. Dopants containing heavy metal atoms are ideal for this purpose, since the large spin–orbit coupling promotes emission from triplet states as discussed earlier.

The first metallophosphorescent dopant to exhibit efficient electroluminescence was platinum(II) octaethylporphyrin, **1**, which gave an internal EL quantum efficiency of 23% (corresponding to an external EL quantum efficiency of 4%) when doped into the widely used EL emissive material $\mathrm{Alq_3}$ ($\mathrm{Alq_3}$ = tris(8-quinolinato)aluminum; see Fig. 3 for structures of some of the common host materials used and which will be referred to in later sections) [27,28]. Over 90% of the energy is transferred from $\mathrm{Alq_3}$, confirming that emission occurs from both singlet and triplet excitons. Judicious choice of host raises the internal EL quantum efficiency to 32% [29]. Unfortunately the long phosphorescence lifetime of PtOEP (~60 μs) results in severe triplet–triplet annihilation at high current (Eq. (5), where *M* represents the molecular dopant) [27].

$$4({}^3M^* + {}^3M^*) \rightarrow {}^1M^* + 3\,{}^3M^* + 4M \quad (5)$$

5. Platinum complexes with bidentate N^C-coordinating ligands

5.1. Homoleptic Pt(N^C)$_2$ complexes

Von Zelewsky and co-workers reported the synthesis of the homoleptic bis-cyclometallated complex Pt(N^C-ppy)$_2$ **2** in 1984, followed by analogues with 2-thienyl-pyridine (thpy) and derivatives, and corresponding complexes with pyrazoles in place of the pyridine rings [30,31]. The more pronounced *trans* effect of the cyclometallated carbon over pyridine accounts for the regioselective formation of the *cis* isomers. Subsequent work revealed that some of these compounds are luminescent in solution at room temperature, e.g. for Pt(N^C-thpy)$_2$, **3**, $\lambda_{\max}$ = 578 nm, τ = 2.2 μs in a PrCN/EtCN mixture [32]. A landmark study of the temperature dependence of several cyclometallated complexes by Barigelletti et al. showed that the energy gap between the emissive state and the higher-energy d–d state in Pt(thpy)$_2$ is of the order of 3700 $\mathrm{cm^{-1}}$, sufficiently large to close it off as a pathway of deactivation at room temperature [33]. Yersin and Donges have carried out detailed studies of the excited state properties of this complex, including very low temperature measurements at 1.3 K in a Shpol'skii matrix, the results of which have been reviewed recently [34].

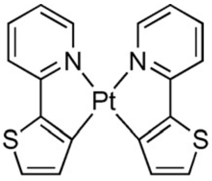

Pt(*N*^*C*-thpy)$_2$

3

Cocchi et al. have investigated the potential of Pt(*N*^*C*-thpy)$_2$ **3** and Pt(N^C-thpy-5-SiMe$_3$)$_2$ **4** as phosphorescent emitters in OLEDs [35,36]. Although these complexes have impressive quantum yields in degassed solution (Φ = 0.35 ± 0.05), they are thermally unstable and hence not amenable to thermal deposition methods of OLED fabrication. However, by spin-casting the emitting layer from a solution containing TPD (to form the host matrix) and Pt complex (as guest), devices could be fabricated successfully {TPD = *N*,*N*′-bis(3-tolyl)-1,1′-biphenyl-4,4′-diamine, Fig. 3}. The TPD host is an excellent sensitiser of the Pt complex, as evident from photoluminescence being observed exclusively from the guest in a 6%-doped film. In the EL device, the external EL efficiency reached 11.5% photon/electron for **4**, considerably superior to the analogous device using PtOEP **1**, due, at least in part, to the excited state lifetime of the cyclometallated complex being an order of magnitude shorter than that of the metalloporphyrin.

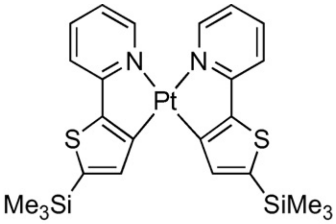

Pt(*N*^*C*-thpy-SiMe$_3$)$_2$

4

5.2. Heteroleptic complexes incorporating the Pt(N^C) unit: [Pt(N^C)X$_2$]$^-$, [Pt(N^C)L$_2$]$^+$ and [Pt(N^C)(LX)]

The formation of the bis-cyclometallated complexes described above normally requires the use of the lithiated ligands, the formation of which is intolerant of many functional groups. In contrast, the introduction of just one N^C-coordinating ligand into the coordination sphere of Pt(II) can normally be accomplished readily upon reaction with simple salts such as $\mathrm{K_2PtCl_4}$, leading to chloro-bridged dimers (Eq. (6)) [37].

$$\mathrm{K_2PtCl_4} + \mathrm{N\hat{C}H} \rightarrow (\mathrm{N\hat{C}})\mathrm{Pt}(\mu\text{-Cl})_2\mathrm{Pt}(\mathrm{N\hat{C}}) \quad (6)$$

The dimers can then be cleaved under mild conditions by L̂L-coordinating diamines or diimines, such as en and bpy, to give [Pt(N^C)(N^N)]$^+$ complexes [38], or by bidentate anionic ligands L̂X such as β-diketonates to give [Pt(N^C)(OÔ)] complexes [39]. The introduction of monodentate ligands can be achieved similarly, leading to complexes such as [Pt(N^C)Cl$_2$]$^-$ [38], [Pt(N^C)(CO)Cl] [40], and [Pt(N^C)(CO)SR] [41].

In such complexes, one might anticipate that the strong ligand field associated with the cyclometallated carbon should favour luminescence by displacing the d–d states to high energy. However, on its own, the ppy or equivalent ligand is not necessarily sufficient to induce RT emission: the so-called ancillary ligands are crucial. For example, the complex [Pt(N^C-ppy)Cl$_2$]$^-$, containing weak-field chloride ligands, is luminescent at 77 K, but not at RT [38]. The strong temperature dependence is attributed to a relatively small energy gap of 1700 cm^{-1} between the lowest emitting ^{3}MLCT state and the upper lying d–d states, the thermally activated population of which can occur at RT, quenching the emission. In contrast, [Pt(ppy)(en)]$^+$, [Pt(ppy)(bpy)]$^+$ and [Pt(bpy)(phen)]$^+$ are luminescent in DMF solution at 293 K, $\lambda_{max} \sim 486$ nm with microsecond lifetimes. The difference is clearly due to the influence of the ancillary NˆN ligands in increasing the ligand field strength at the metal. Direct population of the emissive triplet state is observed as a weak feature at 482 nm for the en complex, for which a $d_{Pt} \rightarrow \pi^*_{(N^\wedge C)}$ ^{3}MLCT assignment is clear-cut. On the other hand, for the bpy and phen complexes, the electrochemical data indicate that the first reduction process is localised on the diimine rather than the NˆC ligand, and a $d_{Pt} \rightarrow \pi^*_{(N^\wedge N)}$ assignment is proposed in these cases [38].

A disadvantage of the above complexes with regard to their potential application to OLEDs would be the fact that they are charged ions. By using LX̂ ligands (i.e. those that offer one neutral and one anionic ligating atom, of which acetylacetonate is a classic example), charge–neutral complexes are accessible which are more appropriate. Thompson et al. have conducted a systematic study of cyclometallated complexes of the form [Pt(NˆC)(OÔ)], where OÔ represents acetylacetonate (acac) or its *t*-butyl analogue dipivaloylmethane (dpm) [39]. Twenty-three different NˆC-coordinating ligands were investigated, including several containing substituents in either the phenyl or the pyridyl rings of ppy, as well as some more extended aromatic structures.

All of the complexes are intensely luminescent in glasses at 77 K, and several – though not all – are also quite strongly emissive in fluid solution at RT. The emission is assigned to states of mixed $d_{Pt}/\pi_{N^\wedge C} \rightarrow \pi^*_{N^\wedge C}$ (MLCT/LC) character on the basis of electrochemical measurements and DFT calculations, which suggest that the HOMO levels in these complexes comprise contributions from both Pt and ligand orbitals while the LUMO is largely localised on the NˆC ligand [39]. Such an assignment is also able to account for the observed trend in emission energies as a function of the ligand substituents. Thus, electron-*withdrawing* F or CF$_3$ substituents on the 4′ and 6′ positions of the *phenyl* ring of ppy induce a blue shift in the emission, as the HOMO is stabilised (Fig. 4). On the other hand, the incorporation of electron-*donating* –OMe or –NMe$_2$ substituents into the *pyridyl* ring raises the LUMO, also resulting in a blue shift. The effects in the two rings are qualitatively additive, allowing quite substantial shifts towards the blue to be obtained (Fig. 4).

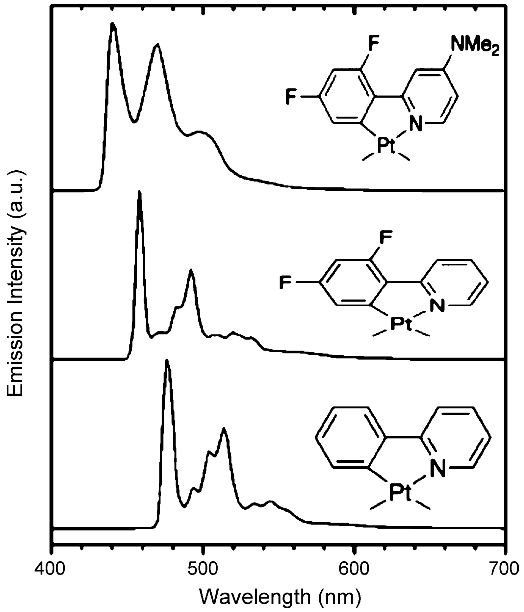

Fig. 4. (From bottom to top) Emission spectra of Pt(ppy)(dpm), **5**, Pt(F$_2$ppy)(dpm), **6-dpm**, and Pt(F$_2$pdmapy)(dpm), **7**, in MeTHF at 77K. The OÔ-chelated dpm ligand is omitted in the partial structures shown. Reprinted with permission from [39]. ©(2002) American Chemical Society.

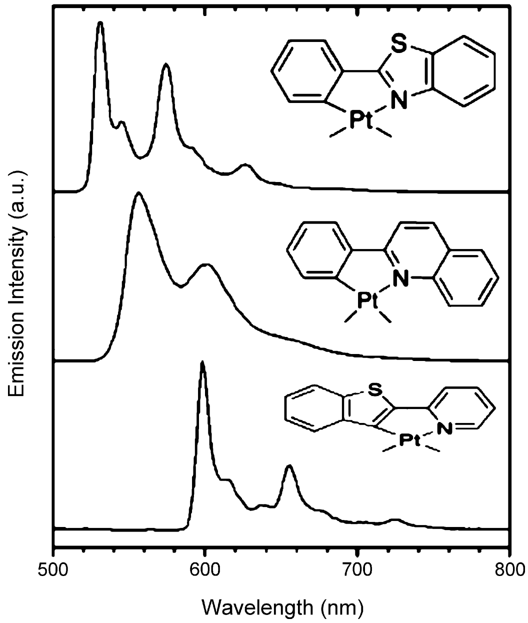

Fig. 5. (From top to bottom) Emission spectra of Pt(bt)(dpm), **8**, Pt(pq)(dpm), **9**, and Pt(btp)(acac), **10**, in MeTHF at 77 K. The OÔ-chelated dpm ligand is omitted in the partial structures shown. Reprinted with permission from [39]. ©(2002) American Chemical Society.

Despite the high energy of the emissive states induced in this way, however, the most blue-shifted complex Pt(F$_2$pdmapy)(dpm) **7**, (Fig. 4, top) is only feebly luminescent at 298 K, $\Phi < 10^{-3}$ {F$_2$pdmapy = 2-(4′,6′-difluorophenyl)-4-(dimethylamino)pyridinato-*N*,$C^{2'}$}. Contrary to the energy gap law, as the energy of emission increases within this series, the room temperature Φ and τ values decrease, possibly due to thermal activation to an MC state or a competing MLCT state on the ancillary β-diketonate that becomes more significant for the higher energy complexes.

Those complexes which have more extended π systems, or more polarisable atoms such as sulfur incorporated into the

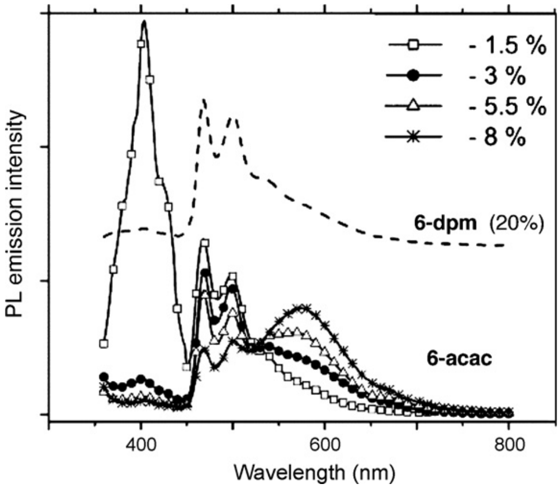

Fig. 6. Photoluminescence spectra of **6-acac** in a CBP film (solid lines) at the doping levels indicated, and of **6-dpm** at 20% in the same matrix (dashed line, displaced vertically for clarity); λ_{ex} = 340 nm. Reprinted with permission from [46]. ©(2002) Royal Society of Chemistry.

ring, have lower oxidation potentials, and their MLCT excited states are correspondingly lower. Fig. 5 illustrates the increasing red-shifts observed upon going from the complex with 2-phenylbenzothiazole (bt) **8**, through 2-phenylquinolyl (pq) **9**, to 2-(2′-benzothiazole)-pyridyl (btp) **10**.

5.3. The role of excimers: white light emitting devices (WOLEDs) using Pt(NˆC) complexes

Sterically unencumbered platinum(II) complexes are frequently susceptible to self-quenching at elevated concentrations, sometimes accompanied by the formation of excimers which may themselves be emissive at lower energy than the isolated monomers. In solution, excimer formation is a diffusion-controlled process involving the interaction of one molecule in its excited state with a second, identical molecule in its ground state. The resulting weakly attractive interaction stabilises the excited state, leading to red-shifted emission compared to the isolated monomer. In the solid state, excimer-like emission can arise if the packing of molecules is appropriate to allow such an interaction, or it may result from aggregation of the molecules in the ground state. The latter includes interactions that involve overlap of the d_{z2} orbitals, which frequently lead to $d\sigma^*(Pt_2) \rightarrow \pi^*$(ligand) (MMLCT) excited states.

Efficient excimer emission is observed in solution for several of the [Pt(NˆC)(OÔ)] complexes described by Thompson et al., and a detailed study of the kinetics and thermodynamics of the monomer/excimer equilibrium for one of them, [Pt(F_2ppy)(acac)], **6-acac**, has been described recently in this journal [42].

From the point of view of OLEDs, the combination of monomer and excimer emission from a single metal complex as dopant may provide an exciting way forward in the development of white light emitting devices (WOLEDs). Whilst high colour-purity dopants are required for RGB displays, the impetus for developing WOLEDs arises from the need for more economical alternatives to conventional incandescent bulbs and fluorescent tubes that currently dominate lighting. The usual way to obtain white light is to use three separate emitters—red, green and blue [43]. However, if all three are combined within a single emitting layer, it can be difficult to control energy transfer from the higher energy blue to the green to the red dye—essentially a short-circuiting of the excited state energy. Segregation of the emitters into different layers can circumvent this problem, but at the expense of necessitating a more elaborate device architecture [44]. Thompson and Forrest have proposed the new approach of using a single phosphorescent dopant emitting simultaneously from monomer and excimer states. Square-planar Pt(II) complexes that emit from excimer or aggregate states are essentially ideal for this purpose [45,46].

Figs. 6 and 7 show results obtained with [Pt(NˆC-F_2ppy)(OÔ)] complexes **6** [46]. Photoluminescence spectra of a CBP host doped with increasing concentrations of [Pt(NˆC-F_2ppy)(acac)], **6-acac**, (Fig. 6) demonstrate that, at a low doping level (1.5%), undesired residual emission from the host is observed in addition to that of the monomeric Pt complex (see Fig. 3 for structure of CBP). As the doping level is increased, the excimer emission rapidly appears, and dominates at levels >8%, which is too low to achieve balanced monomer/excimer emission in a practicable device. The more bulky dpm analogue **6-dpm** shows almost exclusively monomeric emission, even at doping levels of 20%, reflecting the steric inhibition of excimer formation. The complex [Pt(F_2ppy)(OÔ-mhpt)], **6-mhpt**, on the other hand, was found to offer the appropriate level of steric bulk for balanced monomer/excimer emission to be observed at doping levels around 10%, and this behaviour was successfully extrapolated to an EL device (Fig. 7) (mhptH = 6-methyl-2,4-heptanedione). The CIE coordinates of this device (x, y = 0.36, 0.44) are close to those for white light (0.33, 0.33), with a maximal efficiency of 3.3 ± 0.3 photons/electron (7.3 ± 0.7 lm W^{-1}) at 0.5 cd m^{-2} [46].

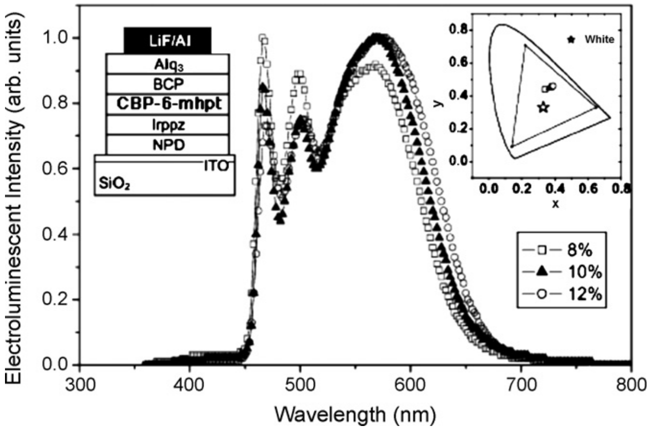

Fig. 7. Electroluminescence spectra and CIE coordinates for **6-mhpt** incorporated into the emissive layer of the multilayer device represented schematically in the inset, at 8, 10 and 12% doping ratios. Reprinted with permission from [46]. ©(2002) Royal Society of Chemistry.

A series of somewhat related complexes have also been reported by Ionkin and co-workers, who used the puckered nature of chelating phosphino alcohols, rather than adding bulk to a planar acac-type ligand, to inibit π–π stacking interactions [47]. For example, solid-state structures reveal not only longer intermolecular Pt–Pt distances on going from **11** through **12**–**13**, but also increasing distortion away from the square-planar geometry; indeed **13** is more correctly termed bow-shaped than square planar: the angle between the mean planes of the constituent rings of the phenylpyridine unit is 19.7°. On the other hand, the plane-to-plane distance reaches a maximum in **12** (4.203 Å compared to 3.504 and 3.533 Å in **11** and **13**, respectively). This effect is reflected in the electroluminescence spectra, where **12** emits at highest energy (540 nm), without apparent contribution from a lower-energy excimer band. In solution, this complex is reported to emit at extraordinarily high energy, (λ_{max} = 405 nm) [47], but in the absence of further photoluminescence data such as quantum yields and lifetimes, it is difficult to place this result in the context of other emissive Pt(II) complexes.

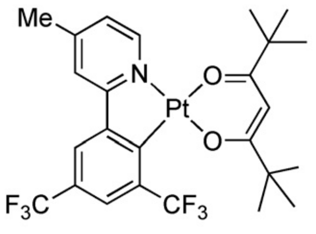

11

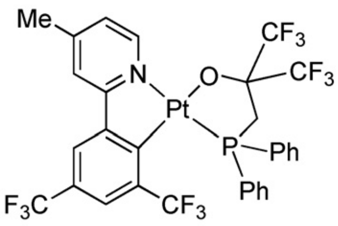

12

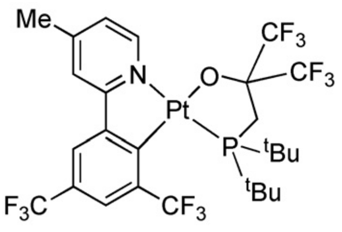

13

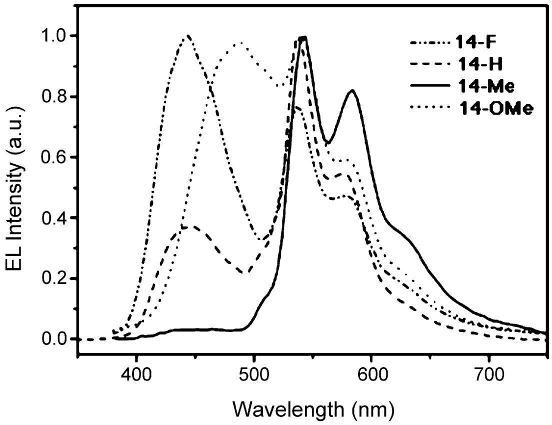

Fig. 8. Electroluminescence spectra of multilayer OLEDs incorporating **14** (R = F, H, Me, OMe) at the 5% doping level within the CBP host emissive layer. Fluorescence and phosphorescence from the dopant is observed, the relative proportions depending on the substituent. Reprinted with permission from [49]. ©(2006) American Chemical Society.

As noted earlier, multilayer configurations are commonly used in devices, consisting of hole-transporting and electron-transporting layers sandwiching the emitting layer, in order to achieve a balanced injection and transport of holes and electrons and to optimise charge recombination within the EL layer. Wong and co-workers have recently prepared multifunctional Pt emitters, which combine, in a single molecule, a Pt(ppy)(acac) emitter with covalently linked oxadiazole and triarylamine units to act as electron- and hole-transporting units, respectively, **14** [48,49]. These compounds are sublimable, and have been used to prepare neat-emissive-layer devices. For example, a device obtained by vacuum-evaporating **14** (R=H) between an ITO/CuPC anode and Ca/Al cathode emits orange-yellow, with maximum luminous efficiency of 1.2 ca A^{-1} and luminance of 1065 cd m^{-2} at 14 V.

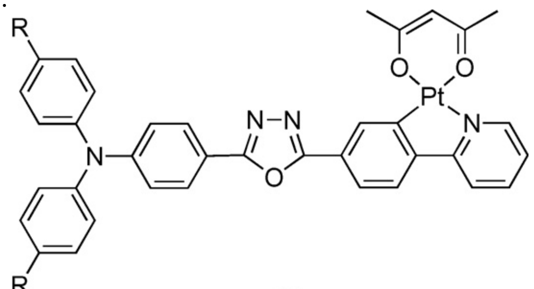

14

In fact, these molecules (**14**) display both fluorescence and phosphorescence in solution; the fluorescence is lowered in energy as the electron-donating character of the substituent R increases, reflecting the predominant contribution of the triarylamine to the HOMO, whilst the phosphorescence energy is essentially invariant. Similar behaviour is observed when these compounds are used as dopants within a CBP emitting layer (Fig. 8). Interestingly, the ratio of fluorescence to phosphorescence in these devices can be controlled according to either the applied voltage (the blue colour intensity increases relative to the orange at increasing voltage), or the concentration of the dopant (intermolecular quenching of triplet excitons at high dopant concentrations leads to an increase in the intensity of the blue component). Under appropriate conditions (concentration and bias voltage), the combination of the two contributions can be tuned to give WOLEDs, complementing the monomer-excimer approach [49].

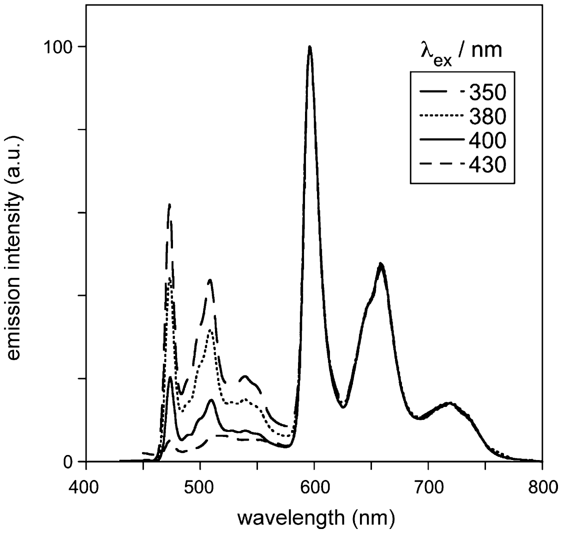

Fig. 9. Emission spectra of **15** (X=H) at 77 K in an EPA glass, showing how the relative intensity of emission from the high-energy *cis* (*Z*) and lower-energy *trans* (*E*) forms varies as a function of the excitation wavelength.

5.4. Further colour tuning with Pt(NˆC) complexes

Guerchais et al., in collaboration with our group, have incorporated stilbene pendants into the 4-position of the pyridyl ring of Pt(NˆC)(OÔ) complexes, **15** [50]. At room temperature, the emission is weak, probably due to a competitive quenching involving *trans–cis* C=C photoisomerisation. ^{1}H NMR spectroscopy confirms the formation of the *cis* isomer upon irradiation. The substituent in the distal aryl ring of the stilbene unit has rather little influence on the emission energy, ($\lambda_{max} \sim 520$ nm), suggesting that, at room temperature, the emissive state is decoupled from the styryl pendant and involves only the Pt(ppy) moiety. A possible explanation is that the RT emission emanates from a conformational form containing a half-twisted –CH=CH– unit that is unconjugated with the ppy ligand [50].

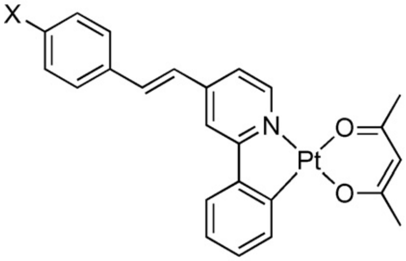

15

X = H, OMe, NO_2, NEt_2

Very different behaviour is observed in a frozen glass at 77 K. Two sets of bands with similar, well-defined vibrational progressions are observed, one in the region 460–560 nm and the second set at substantially lower energy in the range 570–800 nm. These two sets of bands are assigned to the *cis* (*Z*) and *trans* (*E*) isomers, respectively. Evidence in support of this assignment includes the change in relative intensities of the two sets of bands according to the excitation wavelength employed. For example, Fig. 9 shows how the *Z* bands decrease in relative intensity as the excitation wavelength is increased from 350 to 430 nm, which correlates with the longer-wavelength absorption by the *E* isomer. In contrast to the RT

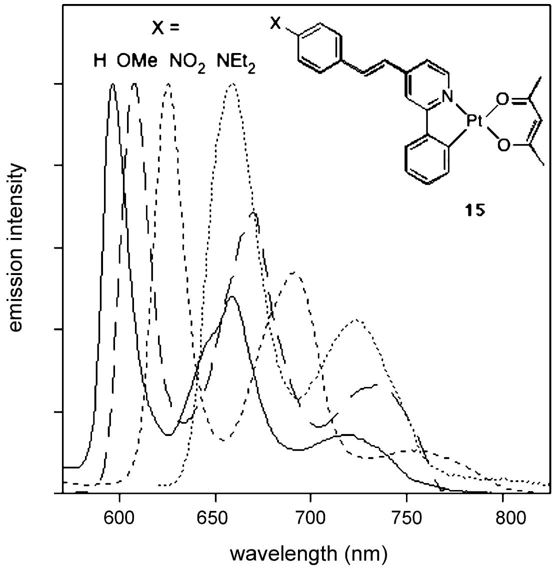

Fig. 10. The long-wavelength region of the emission spectra of **15** (X=H, OMe, NO$_2$ and NEt$_2$) in an EPA glass at 77 K; λ_{ex} = 400 nm.

behaviour, the energy of the *E* bands, but not the *Z* bands, is sensitive to the substituent X (Fig. 10). Interestingly, it can be seen that the introduction of *either* electron-withdrawing *or* electron-donating X substituents shifts the emission further into the red. This somewhat counter-intuitive observation can be understood by considering the localisation of the frontier orbitals. For the complexes with X = –H, –OMe and –NO$_2$, DFT calculations reveal that the HOMO is localised largely on the cyclometallated phenyl ring, the metal and the acac ligand, whereas the HOMO of the amino-substituted complex has additional contribution from the pendant ring. The LUMO varies from being primarily on the distal pendant stilbene ring and substituent (for X = –NO$_2$), to being largely localised on the py-C=C moiety (X = –NR$_2$). Thus, the NO$_2$ group has a much greater influence on the LUMO than on the HOMO, leading to a reduction in the HOMO–LUMO gap and a shift to the red. On the other hand, it is on the HOMO that the NR$_2$ group has the greater effect, introducing a substantial contribution from the pendent ring and additional ILCT character. Again, the net result is that the HOMO–LUMO gap is decreased [50].

An intriguing series of pyrazolate-bridged Pt(N^C) dimers, of the general formula (N^C-F$_2$ppy)Pt(μ-*pz*′)$_2$Pt(N^C-F$_2$ppy), **16** (Fig. 11), where *pz*′ = pyrazolate, 3,5-dimethylpyrazolate, 3-methyl-5-*tert*-butylpyrazolate or 3,5-bis(*tert*-butyl)pyrazolate, have been described recently by Thompson et al. [51]. Single crystal X-ray crystallography reveals that the dimers adopt a boat-like conformation, which brings the platinum centres relatively close together (Fig. 11). Bulky substituents on the pyrazolate bridges force the two Pt(N^C) moieties even closer: the Pt–Pt distances range from 3.3763(7) Å for *pz*′ = pyrazolate to 2.8343(6) Å for 3,5-bis(*tert*-butyl)pyrazolate, and ground state Pt···Pt interactions would be anticipated to be enhanced accordingly. Indeed, in their 77 K emission spectra, the complexes with one and two *tert*-butyl substituents display a broad, structureless, low-energy emission band, typical of a dσ*(Pt$_2$) → π*(ppy) (MMLCT) transition, whereas the other two complexes have vibrationally structured bands at higher energy, typical of the mixed ^{3}MLCT/^{3}LC emission of the Pt(N^C) monomeric complexes. In fluid solution, all four complexes collapse to the MMLCT excited state giving red emission [51].

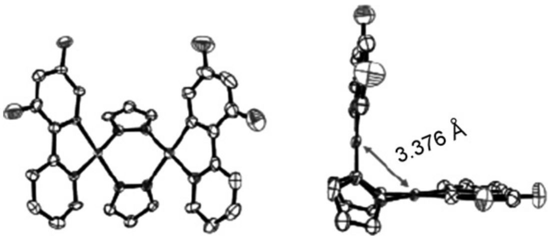

Fig. 11. ORTEP views of (F$_2$ppy)Pt(μ-pz)$_2$Pt(F$_2$ppy), **16**, showing the boat-like conformation that leads to short metal–metal separations. Reprinted with permission from [51]. ©(2005) American Chemical Society.

In the above examples, the “ancillary” ligand lives up to its name: it augments the luminescence efficiency but plays little role in influencing the emission energy, since the excited state is localised on the N^C ligand. In contrast, when 8-hydroxyquinoline or 8-quinolinthiol are introduced as the second bidentate ligand, (e.g. **17a–c** and **18**), emission emanates from low-energy excited states associated with these ligands [52]. Weak emission deep into the red is observed in solution at room temperature, which is shifted increasingly towards the near-infrared upon substitution of the phenyl ring of the quinoline ligand (e.g. λ_{max} increases in the order **17a** < **17b** < **17c**) or upon changing from the quinolinol **17a** to the quinolinthiol **18**. This trend is consistent with an emitting state of ILCT character, with a HOMO localised on the phenolate/thiolate and LUMO on the pyridine ring of the same ligand. In fact, the behaviour is essentially the same as that of homoleptic Pt(quinolinol)$_2$ complexes [53]. The uniformly low quantum yields (Φ_{lum} < 0.01), despite quite long lifetimes on the microsecond timescale, are indicative of low k_r values, and hence a low degree of participation of the metal in the ILCT state.

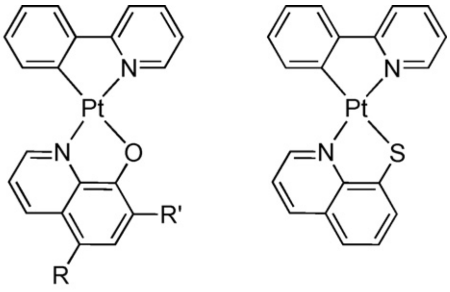

17 a R = R' = H
b R = Cl, R' = H
c R = R' = CH$_3$

18

6. “Pseudo-cyclometallates”: anionic N^N$^-$-coordinating ligands

Bidentate ligands comprising the combination of a pyridine ring and a 5-membered azole ring (pyrazole, imidazole or triazole), have been increasingly investigated in coordination chemistry over recent years [54]. In some cases, for example, 3-(2-pyridyl)pyrazoles, there are two tautomeric forms according to which of the two nitrogen atoms within the azole ring carries the H atom (Fig. 12). If binding to a metal is accompanied by deprotonation, then the anionic ligand is essentially an analogue of a cyclometallating ligand like ppy. For example, a number of charge-neutral iridium(III) complexes with attractive luminescence properties were described by Chi et al. that contain one such anionic N^N$^-$-binding ligand in combination with two N^C-coordinating ligands [55].

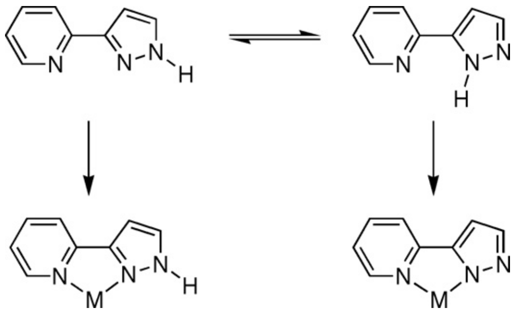

Fig. 12. The tautomeric forms of 3-(2-pyridyl)-pyrazole can allow it to coordinate to a metal M as either a neutral N^N-binding ligand, or as an anionic N^N$^-$ ligand analogous to a cyclometallating N^C ligand.

Recent work by Chi et al. has been exploring the chemistry of such ligands with platinum(II) [56]. They have investigated a number of complexes, such as **19**–**22**, and their studies have revealed some remarkably different emission properties according to subtle changes in the ligands. For example, complexes **19a** and **19b**, which carry a *t*-butyl substituent, are strongly luminescent in degassed solution at room temperature from states of predominant ^{3}MLCT character ($\Phi = 0.82$ and 0.86; $\tau = 2.4$ and $2.1\,\mu s$, respectively). In contrast, the related complexes **20a** and **20b**, and triazole analogues **21** and **22** display only very weak and short-lived emission under the same conditions ($\Phi < 10^{-3}$; $\tau < 10\,ns$), possibly due to severe self-quenching promoting excited state deactivation even in dilute solution. On the other hand, these complexes are brightly emissive in thin solid films at RT, under which conditions the emission probably emanates from an MMLCT d$\sigma^* \rightarrow \pi^*$ state. Support for this assignment includes the columnar stacking arrangement observed in the packing of **20b** in the crystal, with short Pt···Pt contacts of 3.442 Å. This observation contrasts with the displaced arrangement of the molecules found in the structure of **19b**, where Pt···Pt distances are too long for significant interactions of the d_{z2} orbitals. The upshot is that both classes of complexes can be successfully applied in electroluminescent devices when doped into a CBP host; for example, at a 20% doping level, an external quantum efficiency of 6% was observed in a device employing **20a** [56].

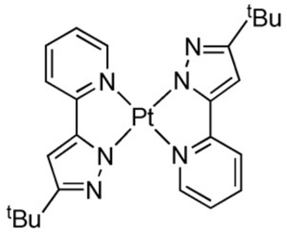

19a

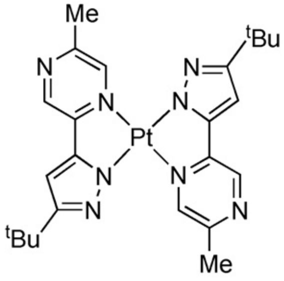

19b

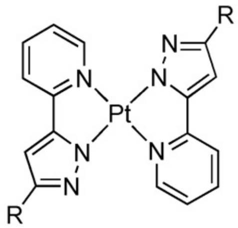

20 **a** R = CF_3 **b** R = C_3F_7

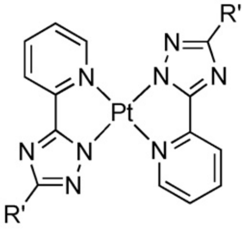

21 R' = ^{t}Bu

22 R' = C_3F_7

More recently, the same group has examined the platinum complexes of a pair of isomeric isoquinolyl-indazole ligands, 1-iqdzH and 3-iqdzH [57]. They contain an isoquinoline unit bound through the 1- or 3-position to the 3-position of an indazole-like moiety in which the usual saturated ring is replaced by a camphor group. These compounds can bind to Pt(II) as neutral ligands, to generate [Pt(N^N-iqdzH)Cl_2] complexes **23** and **24** which – like [Pt(bpy)Cl_2] – are non-emissive. However, further reaction with anionic ligands such as picolinate or 3-trifluoromethyl-5-(2-pyridyl)-pyrazolate is accompanied by deprotonation of the indazolic NH, leading, in the case of picolinate for example, to **25** and **26**. Similarly, deprotonation occurs upon reaction with a second equivalent of the indazole ligand to generate charge–neutral, homoleptic complexes. All of these complexes are luminescent in fluid solution at RT, an effect that can be attributed to the increase in ligand-field strength accompanying the deprotonation. The 1-iqdz complexes give uniformly higher quantum yields and longer lifetimes than the 3-iqdz isomers. This effect, which is most dramatic for the picolinate complexes ($\Phi = 0.64$ and 0.035, $\tau = 8.2$ and $0.85\,\mu s$ for **25** and **26**, respectively, in CH_2Cl_2 at RT), seems to be due primarily to non-radiative rate constants, Σk_{nr}, being substantially smaller for the 1-substituted isomers. For the heteroleptic complexes, but not the homoleptic, the effect is further enhanced by faster radiative rate constants, k_r, for the 1-iqdz isomers, which can be traced back to a higher contribution of metal character to HOMO-1 making the S_0–T_1 transition more allowed [57].

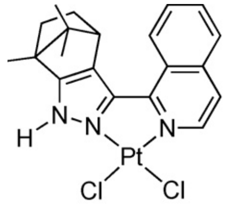

Pt(1-iqdzH)Cl_2

23

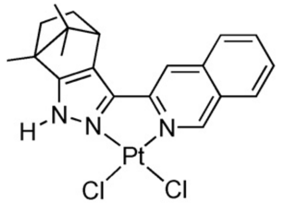

Pt(3-iqdzH)Cl_2

24

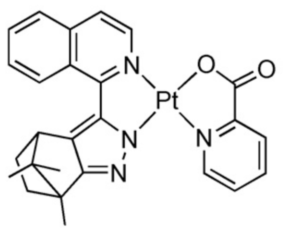

[Pt(1-iqdz)(pic)]

25

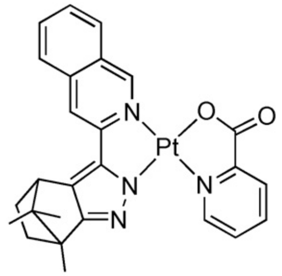

[Pt(3-iqdz)(pic)]

26

7. Pt(N^N^C) complexes

Rigidity generally favours luminescence over non-radiative decay pathways. This rule of thumb applies to platinum complexes just as for any fluorescent molecule. In terms of optimising luminescence efficiencies, therefore, terdentate ligands may offer an advantage over bidentate ligands in that their additional rigidity inhibits the D_{2d} distortion that bis-bidentate complexes can undergo, through twisting of the two planes relative to one another.

Applied to cyclometallated systems, such reasoning naturally suggests that if the cyclometallating ring is incorporated into a terdentate system rather than a bidentate ligand (e.g. NˆNˆC rather than NˆC), then increases in luminescence quantum yields might be anticipated.

Much of the work on complexes comprising platinum(II) bound to NˆNˆC-coordinating ligands has been pioneered by Che and Lai, who have made use of the luminescence of such complexes in a number of applications over the past decade [58]. 6-Phenyl-2,2′-bipyridine (phbpyH) is the simplest such ligand, originally shown by Constable to bind to Pt as an NˆNˆC ligand [59]. The room temperature solution luminescence of [Pt(phbpy)Cl], (**27**, R = H), was assigned by Che to a ^{3}MLCT excited state, λ_{max} = 565 nm, τ = 0.51 μs, ϕ = 0.025 [60]. Self-quenching at elevated concentrations was observed, but there was no evidence for emission from an excimer. The introduction of pendent aryl groups in the 4-position of the central pyridyl ring of **27** (e.g. R = Ph, *p*-Cl–C_6H_4, *p*-Me–C_6H_4, *p*-MeO–C_6H_4–, 3,4,5-$(MeO)_3$–C_6H_2–) augments the quantum yield by factors of 2–3, without significantly changing the emission maximum, suggesting limited electronic communication between the pendent aryl group and the planar phbpy unit [61]. Campagna et al. found that an analogue with R = $C_{12}H_{25}O$–C_6H_4– displays significantly lower-energy emission (λ_{max} = 590 nm), presumably due to the long alkyl chain favouring a conformation that maximises the interaction of the pendant with the phbpy moiety [62].

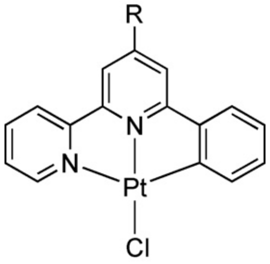

27

In contrast to the solution behaviour, the aryl substituents in Che's study do influence the solid-state emission. The two methoxy-substituted complexes and the parent [Pt(phbpy)Cl] emit at substantially longer wavelengths (665–687 nm) than the other complexes (emission around 600 nm). Moreover, the emission for the former group is shifted to longer wavelengths (700–722 nm) upon cooling the solid to 77 K, whereas the others are blue-shifted. This contrasting behaviour is interpreted in terms of an emissive dσ^*(Pt_2) → π^*(phbpy) MMLCT state for the former group, stabilised upon cooling as the Pt–Pt distance decreases, and d(Pt) → π^*(phbpy) MLCT states for the latter group of complexes [61].

The chloride ligand in [Pt(NˆNˆC)Cl] complexes can be readily displaced by other ligands, which can lead to a change in the nature of the emissive state. For example, the pyridyl adducts $[Pt(phbpy)(py'')]^+$ (py″ = pyridine or 4-aminopyridine) display structured, high-energy emission spectra (λ_{max} 494 nm in MeCN at room temperature), assignable to $^3\pi$–π^* states [63]. In contrast, the 2-aminopyridine analogue **28** emits at substantially lower energy (λ_{max} 534 nm), even though the σ-donating ability of 2-ap is similar to 4-ap. This surprising difference has been interpreted in terms of the *ortho*-NH_2 groups destabilising the Pt dπ orbitals through intramolecular interactions of their lone pairs with the metal centre, an explanation supported by short Pt–N(H_2) distances observed in the crystal structure. It leads to an increase in MLCT character in the emissive state. Essentially, the Pt···N interactions stabilise the "hole" that is formally generated on the metal upon formation of the MLCT state.

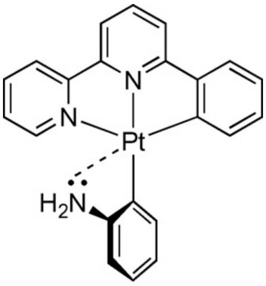

28

Phosphines can also be introduced into the fourth site. Che's group has explored the use of bidentate or terdentate phosphines, of varying length, to bridge between two or even three Pt complexes **29** [61,64,65]. When dpm is used as the bridge (one carbon spacer), low-energy, structureless emission is observed in solution. The bridge holds the two Pt units sufficiently close and in the appropriate face-to-face conformation for Pt···Pt interactions in solution: emission is assigned to the MMLCT excited state. When longer bridges are used (3 or 5 carbon spacers), emission characteristic of the ^{3}MLCT state is restored [61].

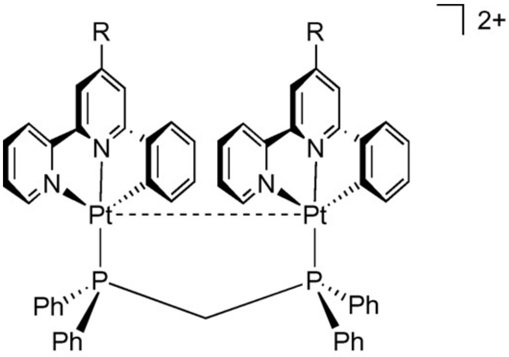

29

Che and co-workers have combined the benefits of terdentate cyclometallation with those associated with acetylide co-ligands discussed in Section 2.2.2. They have carried out a comprehensive study of [Pt(NˆNˆC)(–C≡C–R)] complexes **30**–**32**, in which over 30 derivatives were prepared containing acetylides in the fourth coordination site [66]. Based on the combination of the strong-field cyclometallating carbon, the strong-field acetylide, and the rigidity of the terdentate ligand, high efficiency luminescence would be anticipated and, indeed, all the complexes studied are luminescent in fluid solution, with quantum yields typically in the range 0.05–0.10. The emission wavelengths in solution can be tuned over the range 560–660 nm according to the identity of substituent R and/or the NˆNˆC ligand employed. The thermal stability and sublimability of these complexes renders them appropriate for incorporation into the emissive layer of vapour-deposited OLEDs. EL spectra for devices prepared using **30**–**32** are shown in Fig. 13, from which it can be seen that colour tunability is retained in the device; the device architecture employed is shown in the inset. The highest luminance (9800 cd m^{-2} at 12 V) and external quantum efficiency (η_{ext} = 1.1% at 20 mA cm^{-2}) were achieved using complex **30c** at a 4% doping level within the CBP host. Whilst a somewhat higher efficiency could be obtained by using a 2% ratio of **1** (η_{ext} = 1.6% at 30 mA cm^{-2}), weak emission from the host was observed under these conditions. The generally lower efficiencies and inferior performance observed at higher doping ratios were attributed to aggregate-induced quenching [66].

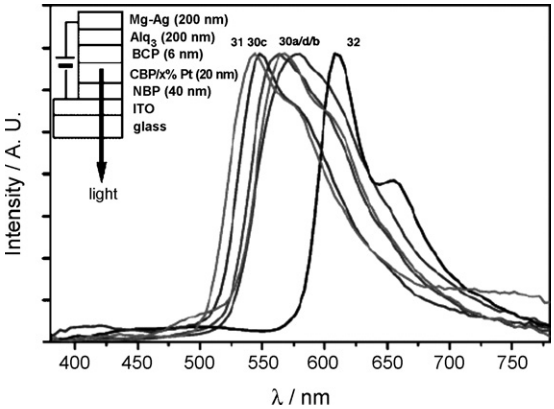

Fig. 13. Electroluminescence spectra for the device structure shown in the inset, using Pt(N^N^C)(–C≡C–R) complexes as the Pt dopant within the CBP host layer. In order of increasing λ_{max}: complexes **31**, **30c**, **30a**, **30d**, **30b**, **32**. Reprinted with permission from [66]. ©(2004) American Chemical Society.

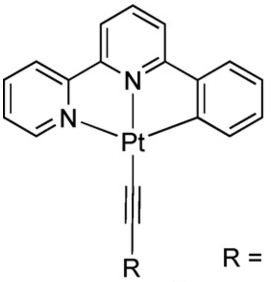

R =

30
- **a** Ph
- **b** p-C_6H_4-Me
- **c** C_6F_5
- **d** ^tBu

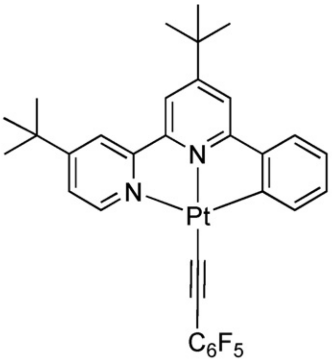

31

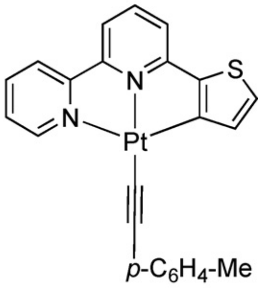

32

Very recently, the same group has reported that N^N^C-coordinated complexes with more extended conjugation in the ligand, comprised of lateral quinolyl and naphthyl units, **33**, display substantially higher luminescence quantum yields than the phbpy analogues; (e.g. for R = –3,5-C_6H_3–$^tBu_2$, Φ = 0.68, λ_{max} = 533 nm in CH_2Cl_2 at RT) [67]. High-performance OLEDs have been fabricated using these chloro complexes, without the need to introduce acetylide co-ligands.

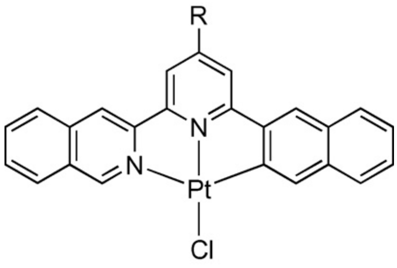

33

Lam et al. have recently described some intriguing results using N^N^C-coordinating ligands in which the lateral N-binding ring is a pyrazole instead of the usual pyridine [68,69]. As in the case of the chloro complexes of the isoquinolyl indazole ligands, **23** and **24**, described in Section 6, the azole ring remains protonated such that the ligand binds as a mono-anionic N^N^C ligand, just like phbpy. However, the pyrazole N–H in the resulting complex, **34** (Fig. 14) can be deprotonated readily, a process that is accompanied by the formation of a dimer, **35**, in which the deprotonated nitrogen atom of each complex has displaced the chloro ligand of the other. Both forms are emissive from ^{3}MLCT states in solution at RT, but the quantum yield of the dimer is considerably superior: Φ_{lum} = 0.14 (in MeCN) and 0.59 (in DMF) for **34** and **35**, respectively [69].

8. Pt(N^C^N) complexes

Our group has been exploring the coordination of platinum(II) to terdentate ligands based on the 1,3-di(2-pyridyl)benzene (dpybH)

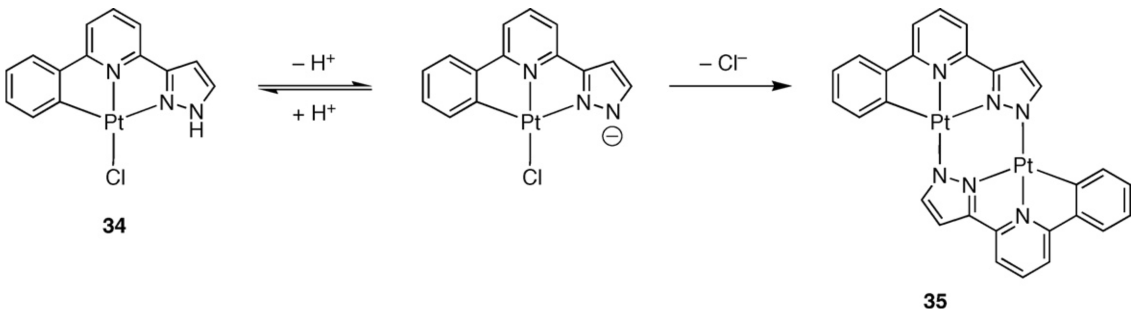

Fig. 14. Complex **34**, containing a pyrazole-based N^N^C-coordinating ligand, undergoes deprotonation of the pyrazole N–H upon treatment with base, to give the dimeric system, **35**.

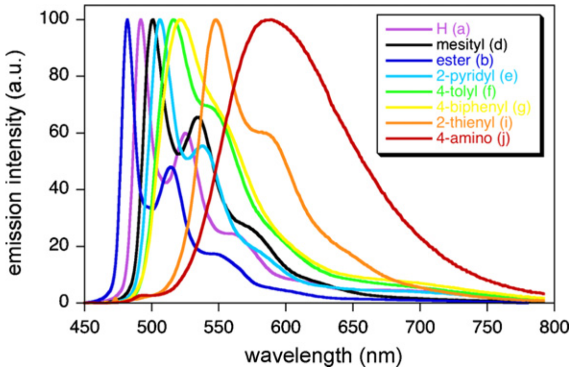

Fig. 15. Emission spectra of N^C^N-coordinated complexes **36** in CH_2Cl_2 at RT, $\lambda_{ex} = 400$ nm.

structure, in which the cyclometallating phenyl ring occupies the central position, hence offering the metal an N^C^N environment. Structurally, this leads to shorter Pt–C bonds than in the isomeric N^N^C systems: X-ray crystallography of a number of Pt(N^C^N) complexes has revealed Pt–C bond lengths of around 1.90 Å, about 0.14 Å shorter than those typically observed for N^N^C complexes. The parent complex [Pt(dpyb)Cl] (**36a**, R = H) is intensely emissive in dilute solution at RT; e.g. $\Phi_{lum} = 0.60$ and $\tau = 7.2\ \mu s$ in deoxygenated dichloromethane [70]. The lifetime at 77 K is the same, within the experimental uncertainty on the measurement, as that at room temperature, indicating that N^C^N coordination is effective at closing off pathways of potential thermally activated non-radiative decay, a result of the strong ligand field. The highly structured profile of the emission spectrum, and the very small Stokes shift between the highest energy emission band and the weak but distinct $S_0 \rightarrow T_1$ absorption band, imply a predominant π–π^* assignment for the emissive state, although theoretical studies using DFT reveal a significant d–π^* component, accounting for the relatively high triplet radiative rate constants [71].

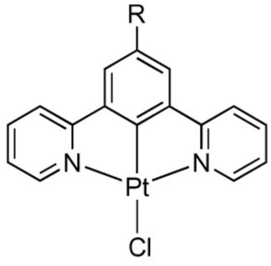

36

a H **b** —CO_2Me **c** —Me

d —mesityl **e** —2-pyridyl **f** —4-tolyl

g —4-biphenyl **h** —3,4-dimethoxyphenyl

i —2-thienyl **j** —C_6H_4-NMe_2

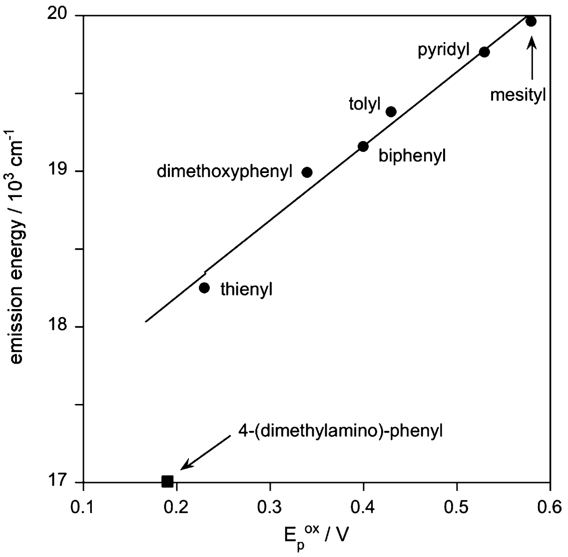

Fig. 16. Correlation of the emission energy E_{em} of aryl-substituted complexes **36** (R = aryl), with the oxidation peak potential measured by cyclic voltammetry in CH_2Cl_2.

The excited state energy is influenced by substituents at the 4-position (R) of the central phenyl ring. For example, the introduction of electron-releasing aryl groups shifts the emission increasingly to the red according to their electron-donating ability (Fig. 15) [72], e.g. λ_{max} increases in the order R = CO_2Me < H < mesityl < Me < 2-pyridyl < 4-tolyl < 4-biphenylyl < 3,4-dimethoxyphenyl < 2-thienyl. The emission energy correlates roughly linearly with the oxidation peak potentials E_p^{ox} of the complexes, with a slope of 4900 cm^{-1} V^{-1} (Fig. 16), whereas there is little difference between the reduction potentials. This suggests that the influence of the substituent is primarily on the HOMO, and that the observed red shift with increasing electron-donating ability reflects an increase in the HOMO level and a LUMO that remains essentially unchanged. Such conclusions are supported by the DFT calculations revealing a major contribution of the phenyl 4-position to the HOMO but not to the LUMO, which, in contrast, is localised predominantly on the pyridyl rings.

The complex with the strongly electron-donating pendant R=–$C_6H_4NMe_2$, **36j**, lies well off the approximately linear E^{em} vs. E_p^{ox} correlation displayed by the other complexes. Its emission band is broad, structureless and displays a high degree of positive solvatochromism, in contrast to the other systems whose energies are insensitive to the solvent. This behaviour is interpreted in terms of a switch in the nature of the lowest-energy excited state from π–π^* to one of primarily intraligand charge-transfer character. Reversible switching between the ILCT and π–π^* states can be induced by simple protonation (Fig. 17). Unusually for transition-metal-based systems, both the ILCT and π–π^* excited states are highly luminescent with comparable quantum yields ($\Phi_{lum} = 0.46$ and 0.40 for the non-protonated and protonated forms, respectively, in degassed dichloromethane).

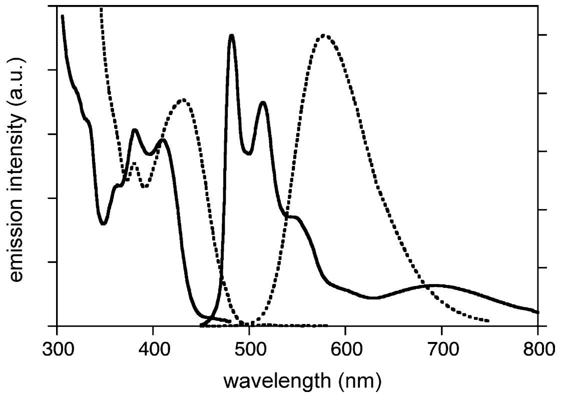

Fig. 17. Emission and excitation spectra of **36j**, R = –C_6H_4–NMe_2 (dotted line) in CH_2Cl_2 at RT (6×10^{-5} M), and of the same solution after addition of trifluoroacetic acid (solid line).

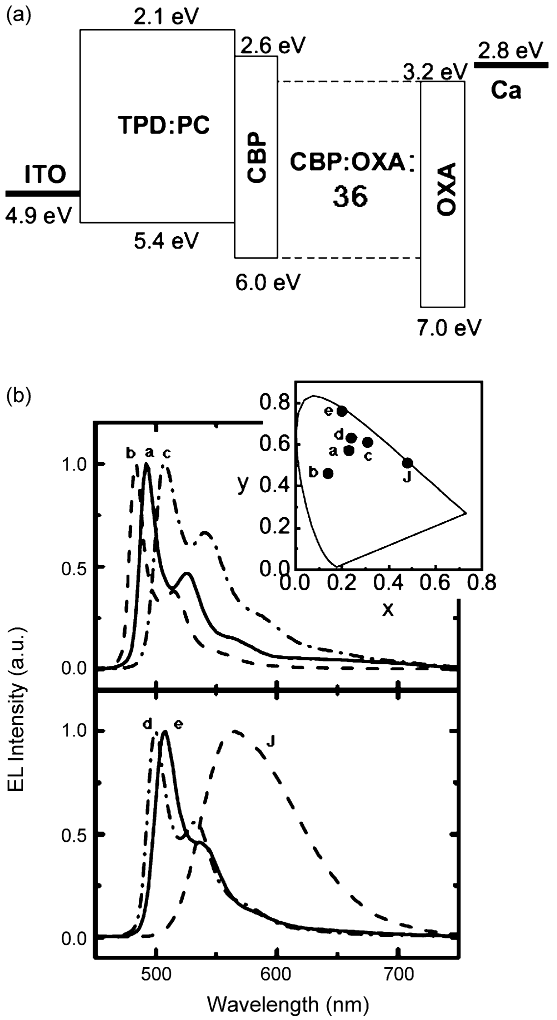

Fig. 18. Devices of structure shown in (a), prepared using some of the complexes of type **36** within the emitting layer (6% by mass), display the EL spectra shown in (b). The corresponding CIE coordinates are shown in the inset. Reprinted with permission from [74]. ©(2007) Wiley-VCH.

The high luminescence quantum yields of this class of complexes renders then particularly attractive as potential OLED phosphors [73,74]. High-efficiency devices have been fabricated by doping them into a CBP host in a multilayer device. The colour tunability according to substituent R is highlighted by the CIE coordinates of the electroluminescence (Fig. 18). External electroluminescence quantum efficiencies of 4–16% photons/electron and luminous efficiencies of 15–40 cd A^{-1} were achieved using this device structure, which were maintained over a 10^4 range in current density without suffering the high-current “roll-off” that is frequently observed [74,75].

8.1. Pt(N^C^N) excimers: near-IR emitting OLEDs and high-efficiency WOLEDS

In solution, the complexes **36a**–**i** efficiently form excimers at elevated concentrations. The excimers, which emit around 700 nm, are unusually intensely emissive, with quantum yields of excimer luminescence estimated to be around 0.35 [76]. In the solid state, the nature of the emission is subtly dependent upon the packing of the molecules, and different polymorphs of a given complex have been isolated that display either monomeric or excimer-like emission. In the case of thin films prepared by evaporation, exclusively excimer-like emission is observed (Fig. 19a). By using a vacuum-evaporated layer of the neat complex, in place of the Pt-doped CBP layer in the device structure shown in Fig. 18, near-infrared emitting electroluminescence devices are obtained (Fig. 19b) displaying remarkably high external quantum efficiencies up to 10.7% photons/electron and light output of 15 mW/cm^2 [76].

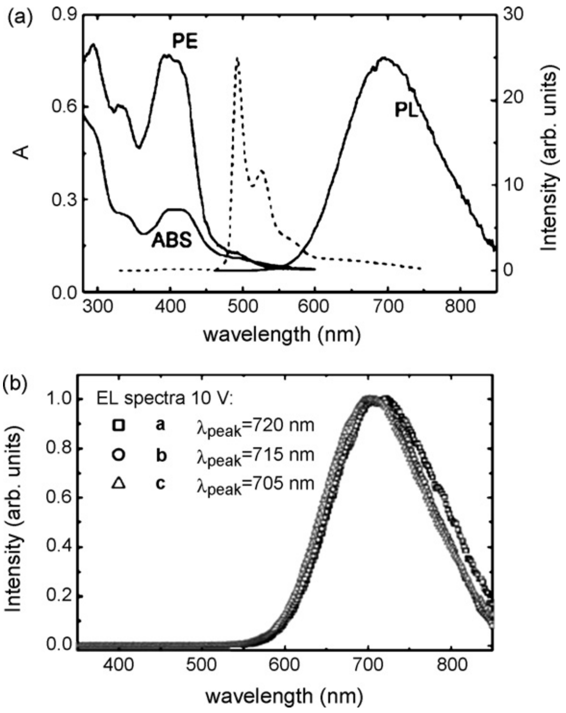

Fig. 19. (a) Absorption (ABS), photoluminescence (PL, λ_{ex} = 350 nm) and photoexcitation (λ_{em} = 650 nm) spectra of a 60-nm thick neat film of **36a**. The PL spectrum of a PC film containing 6 wt.% of **36a** is displayed for comparison (dashed line). (b) Electroluminescence spectra recorded at an applied voltage of 10 V for devices based on the architecture of Fig. 18a, but using neat films of the Pt complex (**36a**–**c**) as the emissive layer. Reprinted with permission from [76]. ©(2007) American Institute of Physics.

As noted earlier, the combination of monomer and excimer emission can offer a means of obtaining single-dopant white light emitters. For the present class of complexes **36**, the high luminescence quantum yields of both the excimer and monomer make such a prospect particularly attractive. Whilst the green and red regions

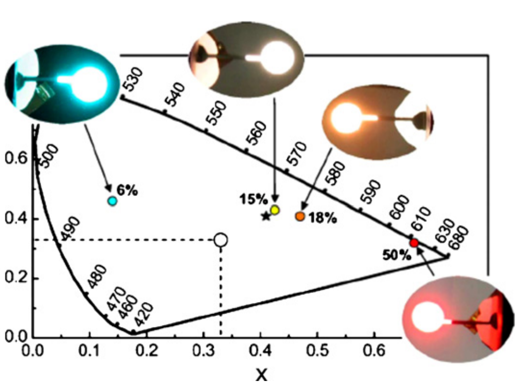

Fig. 20. CIE chromaticity diagram for devices with the architecture shown in Fig. 18a at different doping levels of the Pt complex **36b**. The dots indicate the CIE coordinates of emission from devices prepared with the doping levels shown. Concentrations closest to 15% gave coordinates closest to white (0.33, 0.33) (open circle) and to those found in a typical incandescent lamp (approximately 0.41, 0.41) (asterisk). Reprinted with permission from [77]. ©(2007) American Institute of Physics.

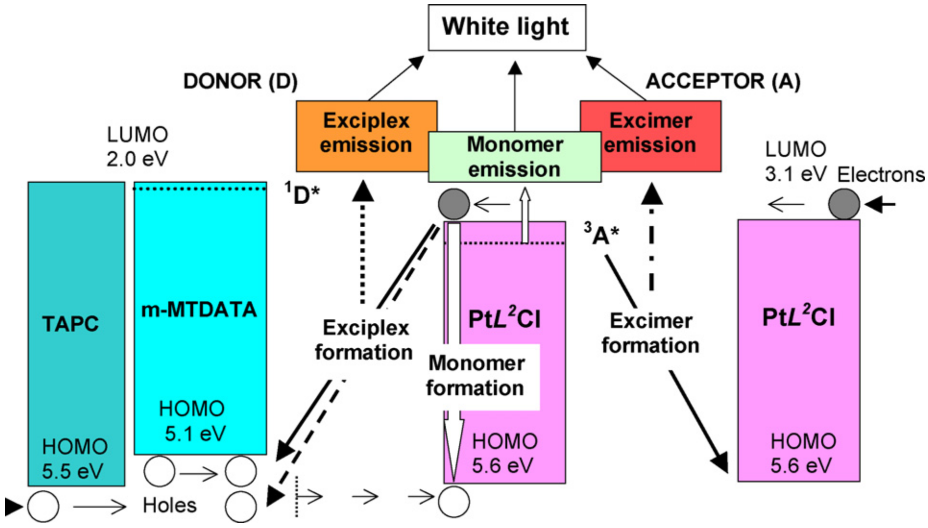

Fig. 21. Generation mechanisms of white light in an OLED based on a hole transporting material (m-MTDATA) acting as an electron donor (D) to an electron acceptor (A) molecule of an organic phosphor (**36b**) mixed in an emissive layer, D:A. The monomer phosphor triplets (^{3}A*), their combination with ground state phosphor acceptor molecules [triplet excimers, ^{3}(AA)*], and excited hetero-dimer [^{3}(DA)*] are generated throughout the emissive layer leading to white light with colour rendering indices CRI up to 90. Reprinted with permission from [79]. ©(2007) Wiley.

are covered well by most of the complexes within the series, the blue component is more limited, being most significant for the ester-substituted complex **36b**. Fig. 20 shows four devices based on the general structure presented earlier (Fig. 18a), in which the doping level of the Pt complex **36b** within the CBP host varies from 6% by mass – where monomer emission predominates giving blue-green emission, to 50% – where the excimer predominates giving red light [77]. At intermediate dopant concentrations, combined monomer + excimer emission leads to “white light”: concentrations of 15% gave CIE coordinates closest to pure white (0.33, 0.33; open circle), being comparable to those found in an incandescent lamp (0.41, 0.41; asterisk).

8.2. *Organic exciplex light emitting devices (EXLEDs) using platinum complexes*

An alternative method of obtaining broad-band emission is to make use of *exciplexes*. An exciplex is an excited complex of an electron donor D and an electron acceptor A, |DA|*, that is dissociative in the ground state, just like an excimer. Indeed, excimers are essentially a special case of an exciplex, in which the two constituent entities are identical. The dissociative property of the exciplex in the ground state leads to a broad featureless emission band, which may be appropriate for WOLEDs. Normally, in the electron-hole recombination process at the electron donor/acceptor interface, only fluorescence from singlet exciplexes is formed. Kalinowski et al. have found that the use of **36b** as a phosphor sensitiser allows the formation of triplet exciplexes, which yield efficient phosphorescence [78]. A device was fabricated using an emissive layer comprised of a star-burst amine hole-transporting donor (m-MTDATA) combined with electron-transporting bathophenanthroline, doped with **36b**, within an electronically inactive polycarbonate (PC) matrix. The heavy Pt atom imposes all charge recombination events on the doped complex to create phosphorescing triplet exciplexes ^{3}|m-MTDATA:**36b**|*. Broad-band electroluminescence peaking at around 620 nm is observed with an external efficiency of 2.4% photon/carrier [78].

The exciplex emission in the above system ($\lambda_{max} \sim 600$ nm) coincides with the region of the spectrum that is not well covered between the monomer and excimer (peaking 500 and 700 nm, respectively) in the WOLED shown in Fig. 20. By combining all three types of emission, better coverage of the visible region should be possible, and hence a new way to improve the efficiency and CIE output of WOLEDs. Kalinowski et al. have been able to demonstrate this principle for the first time using **36b**, as represented schematically in Fig. 21. In the emitting layer, m-MTDATA acts as an electron donor (D) to X as an electron acceptor (A), mixed in a 1:1 ratio. Monomer phosphor triplets, ^{3}A*, their corresponding excimers ^{3}(AA)* formed upon encounter with ground state A, and excited heterodimers—exciplexes ^{3}(DA)*, are generated throughout the emissive layer. A colour rendering index of 90 with an external quantum efficiency of 6.5% photons/electron has been attained in this way [79]. The phenomenon of electro-photoluminescence in organics has also been demonstrated for the first time recently, using **36b** [80].

9. Concluding remarks

In conclusion, this survey has sought to highlight the advances and key conclusions that have been reached over the past decade with regard to optimising the luminescence efficiencies of square-planar platinum(II) complexes. Cyclometallation typically provides an effective means of reducing the rate of non-radiative decay pathways, probably by displacing normally deactivating d–d states to higher energy. Very high solution luminescence quantum yields have been obtained with a number of cyclometallating ligands, and with related systems based on deprotonated azoles. The high quantum yields, thermal stability and sublimability of some of these complexes have made them of particular interest as phosphors or triplet-harvesting agents in OLEDs. High-performance devices have been obtained that are beginning to rival some of the best iridium-based systems. Meanwhile, the propensity of some of the platinum(II) complexes described here to form excimers or aggregates, which emit at longer wavelengths than the isolated monomers, provides a simple strategy for obtaining not only near-IR-emitting devices, but also efficient production of white light using a single dopant. Such interactions are rarely possible for d^6 complexes, and are certain to spur further research into the design and application of platinum(II) complexes in this field.

Acknowledgements

We thank EPSRC and the University of Durham for supporting studies of platinum chemistry in our laboratory. We are grateful to our colleagues Drs. Massimo Cocchi, Valeria Fattori and Dalia Virgili at the C.N.R. Bologna, Italy, and Professor Jan Kalinowski of Gdansk University of Technology, Poland, for an enjoyable and rewarding collaboration on the application of platinum complexes to OLEDs.

References

[1] S.J. Lippard, in: I. Bertini, H.B. Gray, S.J. Lippard, J.S. Valentine (Eds.), Bioinorganic Chemistry, University Science Books, Sausalito, CA, 1994 (Chapter 9).
[2] H.J. Keller (Ed.), Chemistry and Physics of One-Dimensional Metals, Plenum Press, New York, 1977;
J.S. Miller (Ed.), Extended Linear Chain Compounds, Plenum Press, New York, 1982.
[3] V.H. Houlding, M. Miskowski, Coord. Chem. Rev. 111 (1991) 145;
V.H. Houlding, M. Miskowski, Inorg. Chem. 28 (1989) 1529.
[4] For a recent review, see:
J.A.G. Williams, Top. Curr. Chem. 281 (2007) 205.
[5] R.C. Evans, P. Douglas, C.J. Winscom, Coord. Chem. Rev. 250 (2006) 2093.
[6] M. Montalti, A. Credi, L. Prodi, M.T. Gandolfi, Handbook of Photochemistry, 3rd ed., Taylor & Francis, Boca Raton, FL, 2006.
[7] For a recent study of the ultrafast processes in a set of platinum acetylide complexes:
E.O. Danilov, I.E. Pomestchenko, S. Kinayyigit, P.L. Gentili, M. Hissler, R. Ziessel, F.N. Castellano, J. Phys. Chem. A 109 (2005) 2465.
[8] For example, mixed singlet and triplet emission from an ILCT state has been observed in a platinum(II) terpyridyl complex appended with a remote pyrenyl substituent:
J.F. Michalec, S.A. Bejune, D.R. McMillin, Inorg. Chem. 39 (2000) 2708.
[9] V.M. Miskowski, V.H. Houlding, C.-M. Che, Y. Wang, Inorg. Chem. 28 (1989) 1529.
[10] D. Eastwood, M. Gouterman, J. Mol. Spectrosc. 35 (1970) 359.
[11] H.-K. Yip, L.-K. Cheng, K.-K. Cheung, C.-M. Che, J. Chem. Soc., Dalton Trans. (1993) 2933.
[12] D.R. McMillin, J.J. Moore, Coord. Chem. Rev. 229 (2002) 113.
[13] J.F. Michalec, S.A. Bejune, D.G. Cuttell, G.C. Summerton, J.A. Gertenbach, J.S. Field, R.J. Haines, D.R. McMillin, Inorg. Chem. 40 (2001) 2193.
[14] C.-M. Che, K.-T. Wan, L.-Y. He, C.-K. Poon, V.W.-W. Yam, J. Chem. Soc. Chem. Commun. (1989) 943.
[15] M.H. Wilson, L.P. Ledwaba, J.S. Field, D.R. McMillin, Dalton Trans. (2005) 2754.
[16] C.-W. Chan, L.-K. Cheng, C.-M. Che, Coord. Chem. Rev. 132 (1994) 87.
[17] M. Hissler, W.B. Connick, D.K. Geiger, J.E. McGarrah, D. Lipa, R.J. Lachicotte, R. Eisenberg, Inorg. Chem. 39 (2000) 447.
[18] C.E. Whittle, J.A. Weinstein, M.W. George, K.S. Schanze, Inorg. Chem. 40 (2001) 4053.
[19] V.W.-W. Yam, R.P.-L. Tang, K.M.-C. Wong, K.-K. Cheung, Organometallics 20 (2001) 4476.
[20] Q.-Z. Yang, L.-Z. Wu, Z.-X. Wu, L.-P. Zhang, C.-H. Tung, Inorg. Chem. 41 (2002) 5653.
[21] I.E. Pomestchenko, C.R. Luman, M. Hissler, R. Ziessel, F.N. Castellano, Inorg. Chem. 42 (2003) 1394.
[22] F. Hua, S. Kinayyigit, J.R. Cable, F.N. Castellano, Inorg. Chem. 44 (2003) 471;
F. Hua, S. Kinayyigit, J.R. Cable, F.N. Castellano, Inorg. Chem. 45 (2006) 4304.
[23] X.-J. Liu, J.-K. Feng, J. Meng, Q.-J. Pan, A.-M. Ren, X. Zhou, H.-X. Zhang, Eur. J. Inorg. Chem. (2005) 1856.
[24] F.N. Castellano, I.E. Pomestchenko, E. Shikhova, F. Hua, M.L. Muro, N. Rajapakse, Coord. Chem. Rev. 250 (2006) 1819.
[25] For an introduction to the principles of OLEDs and their operation, see, for example:
L.S. Hung, C.H. Chen, Mater. Sci. Eng. R 39 (2002) 143.
[26] (a) D. Hertel, S. Setayesh, H.G. Nothofer, U. Scherf, K. Müllen, H. Bässler, Adv. Mater. 13 (2001) 65;
(b) J.S. Wilson, A. Köhler, R.H. Friend, M.K. Al-Suti, M.R.A. Al-Mandhary, M.S. Khan, P.R. Raithby, J. Chem. Phys. 113 (2000) 7627.
[27] M.A. Baldo, D.F. O'Brien, Y. You, A. Shoustikov, S. Sibley, M.E. Thompson, S.R. Forrest, Nature 395 (1998) 151.
[28] M.E. Thompson, P.E. Burrows, S.R. Forrest, Curr. Opin. Solid State Mater. Sci. 4 (1999) 369.
[29] D.F. O'Brien, M.A. Baldo, M.E. Thompson, S.R. Forrest, Appl. Phys. Lett. 74 (1999) 442.
[30] L. Chassot, E. Müller, A. von Zelewsky, Inorg. Chem. 23 (1984) 4249.
[31] L. Chassot, A. von Zelewsky, Inorg. Chem. 26 (1987) 2814.
[32] M. Maestri, D. Sandrini, V. Balzani, L. Chassot, P. Jolliet, A. von Zelewsky, Chem. Phys. Lett. 122 (1985) 375.
[33] F. Barigelletti, D. Sandrini, M. Maestri, V. Balzani, A. von Zelewsky, L. Chassot, P. Jolliet, U. Maeder, Inorg. Chem. 27 (1988) 3644.
[34] H. Yersin, D. Donges, Top. Curr. Chem. 214 (2001) 81.
[35] M. Cocchi, D. Virgili, C. Sabatini, V. Fattori, P. Di Marco, M. Maestri, J. Kalinowski, Synthetic Metals 147 (2004) 253.
[36] M. Cocchi, V. Fattori, D. Virgili, S. Sabatini, P. Di Marco, M. Maestri, J. Kalinowski, Appl. Phys. Lett. 84 (2004) 1052.
[37] D.S.C. Black, G.B. Deacon, G.L. Edwards, Aust. J. Chem. 47 (1994) 217.
[38] P.-I. Kvam, M.V. Puzyk, K.P. Balashev, J. Songstad, Acta Chem. Scand. 49 (1995) 335.
[39] J. Brooks, Y. Babayan, S. Lamansky, P.I. Djurovich, I. Tsyba, R. Bau, M.E. Thompson, Inorg. Chem. 41 (2002) 3055.
[40] M.M. Mdleleni, J.S. Bridgewater, R.J. Watts, P.C. Ford, Inorg. Chem. 34 (1995) 2334.
[41] Y.A. Kovelenov, A.J. Blake, M.W. George, P. Matousek, M.Ya. Mel'nikov, A.W. Parker, X.-Z. Sun, M. Towrie, J.A. Weinstein, Dalton Trans. (2005) 2092.
[42] B. Ma, P.I. Djurovich, M.E. Thompson, Coord. Chem. Rev. 249 (2005) 1501.
[43] (a) J. Kido, H. Shionoya, K. Nagai, Appl. Phys. Lett. 67 (1995) 2281;
(b) Y. Kawamura, S. Yanagida, S.R. Forrest, Appl. Phys. Lett. 92 (2002) 87.
[44] (a) J. Kido, M. Kimura, K. Nagai, Science 267 (1995) 1332;
(b) B. D'Andrade, M. Thompson, S. Forrest, Adv. Mater. 14 (2002) 147.
[45] B.W. D'Andrade, J. Brooks, V. Adamovich, M.E. Thompson, S.R. Forrest, Adv. Mater. 14 (2002) 1032.
[46] V. Adamovich, J. Brooks, A. Tamayo, A.M. Alexander, P.I. Djurovich, B.W. D'Andrade, C. Adachi, S.R. Forrest, M.E. Thompson, New J. Chem. 26 (2002) 1171.
[47] A.S. Ionkin, W.J. Marshall, Y. Wang, Organometallics 24 (2005) 619.
[48] W.-Y. Wong, Z. He, S.-K. So, K.-L. Tong, Z. Li, Organometallics 24 (2005) 4079.
[49] Z. He, W.-Y. Wong, X. Yu, H.-S. Kwok, Z. Lin, Inorg. Chem. 45 (2006) 10922.
[50] B. Yin, F. Niemeyer, J.A.G. Williams, J. Jiang, A. Boucekkine, L. Toupet, H. Le Bozec, V. Guerchais, Inorg. Chem. 45 (2006) 8584.
[51] B. Ma, J. Li, P.I. Djurovich, M. Yousufuddin, R. Bau, M.E. Thompson, J. Am. Chem. Soc. 127 (2005) 28.
[52] N.M. Shavaleev, H. Adams, J. Best, R. Edge, S. Navaratnam, J.A. Weinstein, Inorg. Chem. 45 (2006) 9410.
[53] R. Ballardini, M.T. Indelli, G. Varani, C.A. Bignozzi, F. Scandola, Inorg. Chim. Acta 31 (1978) L423.
[54] For a recent example, see:
S.P. Argent, H. Adams, T. Riis-Johannessen, J.C. Jeffery, L.P. Harding, W. Clegg, R.W. Harrington, M.D. Ward, Dalton Trans. (2006) 4996.
[55] C.-H. Yang, S.-W. Li, Y. Chi, Y.-M. Cheng, Y.-S. Yeh, P.-T. Chou, G.-H. Lee, C.-H. Wang, C.-F. Shu, Inorg. Chem. 44 (2005) 7770.
[56] S.-Y. Chang, J. Kavitha, S.-W. Li, C.-S. Hsu, Y. Chi, Y.-S. Yeh, P.-T. Chou, G.-H. Lee, A.J. Carty, Y.-T. Tao, C.-H. Chien, Inorg. Chem. 45 (2006) 137.
[57] S.-Y. Chang, J. Kavitha, J.-Y. Hung, Y. Chi, Y.-M. Cheng, E.Y. Li, P.-T. Chou, G.-H. Lee, A.J. Carty, Inorg. Chem. 46 (2007) 7064.
[58] S.-W. Lai, C.-M. Che, Top. Curr. Chem. 241 (2004) 27.
[59] E.C. Constable, R.P.G. Henney, T.A. Leese, D.A. Tocher, J. Chem. Soc., Dalton Trans. (1990) 443;
E.C. Constable, R.P.G. Henney, T.A. Leese, D.A. Tocher, J. Chem. Soc. Chem. Commun. (1990) 513.
[60] T.-C. Cheung, K.-K. Cheung, S.-M. Peng, C.-M. Che, J. Chem. Soc., Dalton Trans. (1996) 1645.
[61] S.-W. Lai, M.C.-W. Chan, T.-C. Cheung, S.-M. Peng, C.-M. Che, Inorg. Chem. 38 (1999) 4046.
[62] F. Neve, A. Crispini, S. Campagna, Inorg. Chem. 36 (1997) 6150.
[63] J.H.K. Yip, S.J.J. Vittal, Inorg. Chem. 39 (2000) 3537.
[64] W. Lu, N. Zhu, C.-M. Che, Chem. Commun. (2002) 900.
[65] W. Lu, M.C.-W. Chan, N. Zhu, C.-M. Che, C. Li, Z. Hui, J. Am. Chem. Soc. 126 (2004) 7639.
[66] W. Lu, B.-X. Mi, M.C.-W. Chan, Z. Hui, C.-M. Che, N. Zhu, S.-T. Lee, J. Am. Chem. Soc. 126 (2004) 4958.
[67] S.C.F. Kui, I.H.T. Sham, C.C.C. Cheung, C.-W. Ma, B. Yan, N. Zhu, C.-M. Che, W.-F. Fu, Chem. Eur. J. 13 (2007) 417.
[68] C.-K. Koo, B. Lam, S.-K. Leung, M.H.-W. Lam, W.-Y. Wong, J. Am. Chem. Soc. 128 (2006) 16434.
[69] C.-K. Koo, Y.-M. Ho, C.-F. Chow, M.H.-W. Lam, T.-C. Lau, W.-Y. Wong, Inorg. Chem. 46 (2007) 3603.
[70] J.A.G. Williams, A. Beeby, E.S. Davies, J.A. Weinstein, C. Wilson, Inorg. Chem. 42 (2003) 8609.
[71] W. Sotoyama, T. Satoh, H. Sato, A. Matsuura, N. Sawatari, J. Phys. Chem. A 109 (2005) 9760.
[72] S.J. Farley, D.L. Rochester, A.L. Thompson, J.A.K. Howard, J.A.G. Williams, Inorg. Chem. 44 (2005) 9690.
[73] W. Sotoyama, T. Satoh, N. Sawatari, H. Inoue, Appl. Phys. Lett. 86 (2005) 153505.
[74] M. Cocchi, D. Virgili, V. Fattori, D.L. Rochester, J.A.G. Williams, Adv. Funct. Mater. 17 (2007) 285.
[75] J. Kalinowski, M. Cocchi, D. Virgili, V. Fattori, J.A.G. Williams, Chem. Phys. Lett. 432 (2006) 110.
[76] M. Cocchi, D. Virgili, V. Fattori, J.A.G. Williams, J. Kalinowski, Appl. Phys. Lett. 90 (2007) 023506.
[77] M. Cocchi, J. Kalinowski, D. Virgili, V. Fattori, S. Develay, J.A.G. Williams, Appl. Phys. Lett. 90 (2007) 163508.
[78] D. Virgili, M. Cocchi, V. Fattori, C. Sabatini, J. Kalinowski, J.A.G. Williams, Chem. Phys. Lett. 433 (2006) 145.
[79] J. Kalinowski, M. Cocchi, D. Virgili, V. Fattori, J.A.G. Williams, Adv. Mater. 19 (2007) 4000.
[80] J. Kalinowski, M. Cocchi, D. Virgili, V. Fattori, J.A.G. Williams, Chem. Phys. Lett. 447 (2007) 279.